PERGAMON

International Journal of Multiphase Flow 25 (1999) 599–637

International Journal of Multiphase Flow

Two-point description of two-fluid turbulent mixing—I. Model formulation

M.J. Steinkamp [1], T.T. Clark *, F.H. Harlow

Fluid Dynamics Group, T-3, Theoretical Division, Los Alamos National Laboratory, Mail Stop/B216, Los Alamos, NM 87545, USA

Received 24 March 1996; received in revised form 20 October 1998

Abstract

We describe a two-point spectral transport approach to the investigation of fluid instability, generalized turbulence, and the interpenetration of fluids across an interface. The technique also applies to a single fluid with large variations in density. Departures of fluctuating velocity components from the local mean are far subsonic, but the mean Mach number can be large. This work is focused on flows with large variations in fluid density (e.g. two-field fluid interpenetration). The starting point for analysis is the set of Navier–Stokes equations, for which we assume relevance in our investigations, even in the presence of sharp density variations between fluids. Models for two-field analysis with drag representations for momentum exchange can also be used and are discussed previously. In this work departures from mean flow are included in the stochastic concept of turbulence. Reynolds decomposition into mean and fluctuating parts is carried out in the spirit of this generalized concept, which is meaningful despite arbitrariness as to which scales are identified as mean flow and which are identified as fluctuations. This spectral formulation motivates a novel description of the global effects of pressure due to incompressibility. We discuss its derivation and the modifications this 'nonlocal' formulation has on the turbulence spectra. We also discuss the consequences of spectral self-similarity exhibited by this model. This identification of spectral self-similarity in a circumstance of inhomogeneous, variable density turbulence is novel.

Keywords: Spectral turbulence transport model; Inhomogeneous turbulence; Variable density turbulence; Turbulent mixing; Interfacial instability; Two-phase turbulence; Rayleigh–Taylor instability; Two-phase flow

* Corresponding author. Tel.: +1-505-665-4858; e-mail: ttc@lanl.gov.

[1] Present address: Engine Research, Tech Center F, Caterpillar Inc., Peoria, IL 61656-1875, USA

0301-9322/99/$ - see front matter
PII: S0301-9322(98)00064-0

1. Introduction

Turbulence occurs in many circumstances of fluid flow, being driven or sustained by the conversion of large-scale mean flow energy to intermediate-scale fluctuations and dissipated by the entropy-increasing process of cascade to small scales, ultimately to the molecular level where it is manifested in the form of heat.

For a comprehensive overview of the evolution of turbulence modeling, the reader is referred to Markatos (1986) and Launder and Spalding (1972). Additional comments on single-point, second-order closures are given by Launder (1990). Once the Navier–Stokes equations are decomposed into mean and fluctuating parts and ensemble averaged, the simplest way to close the Reynolds stress tensor is to use a simple algebraic expression that relates the turbulence to the mean field. The most popular of these types of models are those that use Prandtl's mixing length hypothesis (Anderson et al., 1984; Bradshaw et al., 1981). However, since these types of models do not transport the turbulence variables, they quickly break down in situations with flow transients and are only useful for flows in which the total effect of the turbulence on the mean flow is small.

A single-point, two-equation K–ϵ transport model for constant density flows was first proposed by Harlow and Nakayama (1967, 1968). Variants of this model have been proposed by other researchers, including Jones and Launder (1972, 1973), Chien (1982), and Nagano and Hishida (1987). Other two-equation models exist such as models that transport the product of K and a turbulent length scale instead of ϵ (Ng and Spalding, 1972), and models that transport the second moment of the vorticity fluctuation instead of ϵ (Saffman, 1970; Saffman and Wilcox, 1974; Ilgebusi and Spalding, 1985).

Second order, two-equation transport models (Rotta, 1951; Daly and Harlow, 1970; Hanjalic and Launder, 1972) transport the full R_{ij} tensor as opposed to only its trace, where K is equal to half the trace of R_{ij}. In contrast to the K–ϵ turbulence model, transport of the full tensor enables a more faithful description of anisotropic flows. Variable density extensions to these models (Besnard et al., 1987; Andronov et al., 1982) transport auxiliary terms such as a mass-fluxing velocity and a density-density correlation.

The multi-scale model of Hanjalic et al. (1980) transports R_{ij} and ϵ at both the energy containing length scales and the energy cascade length scales. This approach uses multiple length scales to represent the dynamics of the turbulent kinetic energy spectrum of flows which depart from spectral equilibrium.

In spectral turbulence transport models, an exact but unclosed Reynolds stress transport equation is derived for two points in space. The equations are Fourier transformed with respect to the separation variable and then angularly integrated in k-space. The resulting formulation implicitly contains length scales associated with turbulence, thus alleviating the necessity for an ad hoc formulation of a transport equation for ϵ. Strategies for closing the triple correlations include the work of Kovasznay (1948) and Heisenberg (1948), the diffusion approximation type model of Leith (1967), the quasi-normal models introduced independently by Chou (1940) and Millionshikov (1941) and advanced through the work of Proudman and Reid (1954), Tatsumi (1957), O'Brien and Francis (1962), Ogura (1963), Orszag (1970), Leith (1971), and André and Lesieur (1977). More sophisticated families of closures exist in the direct interaction approximation (DIA) of Kraichnan (1958, 1959, 1964,

1965), and the test field model (TFM) of Kraichnan (1971, 1972). The models of Kovasznay, Heisenberg, and Leith treat the transfer of energy in k-space as a local (differential) process, while the rest of the previously mentioned spectral models treat the triadic interactions in k-space as nonlocal (integral) phenomena. Kraichnan and Spiegel (1962) showed that the diffusive-type closures can be viewed as a local-transfer limit of the nonlocal models.

Other two-point constant density turbulence transport models include the forms of EDQNM proposed by Cambon (1979), Cambon et al. (1981), Bertoglio (1982), and the diffusion approximation proposed by Besnard et al. (1996). Bertoglio and Jeandel (1987) apply a spectral closure (EDQNM) for boundary layer calculations of constant density flow. Jeandel et al. (1978) and Besnard et al. (1996) demonstrate the integration of a spectral model over k-space by assuming self-similar form functions in k-space. This integration reduces the spectral model to a single-point model, i.e. a K–ϵ type of model. Jeandel et al. applied this strategy to both homogeneous and inhomogeneous turbulence. Clark and Zemach (1995) used the spectral transport model of Besnard et al. (1996) to examine constant density anisotropic flows and the spectral behavior of return to isotropy. Clark and Spitz (1995) have developed a spectral transport model for homogeneous variable density flows, and Besnard et al. (1995) have suggested extensions of the work of Clark and Spitz (1995) and Besnard et al. (1996) for the inhomogeneous variable density case.

The spectral turbulence transport model developed herein for inhomogeneous variable density flows is by no means the most mathematically sophisticated when compared with other spectral transport models. This model does, however, purport to capture much essential physics in the generalized circumstance of the variable density inhomogeneous flow. Due to the implicit assumption of spectral equilibrium inherent to all single-point turbulence transport models, a two-point model can more adequately represent mean flow transients that result in departures from spectral equilibrium than can a one-point model.

Our goal is to investigate the turbulence by means of extended transport approaches, using two-point (spectral) techniques. In a subsequent paper (part II of these articles which will hereafter be referred to as Article II), we seek 'generic' spectral forms by which to describe the turbulence structure, especially in circumstances of inhomogeneous, anisotropic flows. These functions may be exact or approximate, depending on circumstances to be described below. They are usually revealed in greatest clarity under circumstances that are described by self-similar combinations of the physical and spectral variables, but they may also occur to a significant level of approximation in localized regions that are continually approaching self-similarity despite the shifting nature of the mean-flow drive.

Reynolds decomposition and ensemble averaging of the Navier–Stokes equations, using mass-weighted averages, leads to an unclosed hierarchy of transport equations for correlations at all orders. Written for covariant statistics at a single point in space and supplemented by closure derivations or assumptions, the results have proved useful for describing numerous circumstances of two-fluid turbulence (Andronov et al., 1982; Besnard et al., 1987). (The model proposed by Besnard et al. (1987) is hereafter referred to as the BHR model.) There are, however, some significant elements missing from this approach.

A clue to these missing elements lies in considering the much better known turbulence transport equations for constant-density fluid flow. It has long been recognized that a single-point transport equation for Reynolds stress must be supplemented by a transport equation

for an auxiliary quantity, often chosen to be the dissipation tensor, ϵ_{ij}, or its contraction, ϵ. Previously identified (Daly and Harlow, 1970) as the Reynolds-stress sink caused by molecular viscosity, ϵ is more accurately associated with the cascade flux of energy from low to high wave numbers. Recognizing the necessity for a transport equation of this dissipation tensor provides a further motivation for considering a two-point generalization of the Reynolds stress, from which we can derive the spectral transport equations by Fourier transformation. This spectral representation does not require a supplemental transport equation for scale because it describes the continuously evolving distribution of Reynolds stress across all wave numbers. In particular it confirms the interpretation of ϵ as the flux from the dominant lower-wave-number parts of the spectrum through a more-or-less inertial (or Kolmogorov) middle range to high wave numbers. Viscous dissipation may occur at even higher wave numbers at a rate that is not necessarily in equilibrium with the cascade flux. A transport equation for ϵ can be derived as a moment of the full spectral equations provided that an appropriate spectral form can be discovered for the spectral tensor, as discussed below.

With large density differences in the fluid, the spectral analysis becomes much more complicated, especially because we include density variations that arise from the

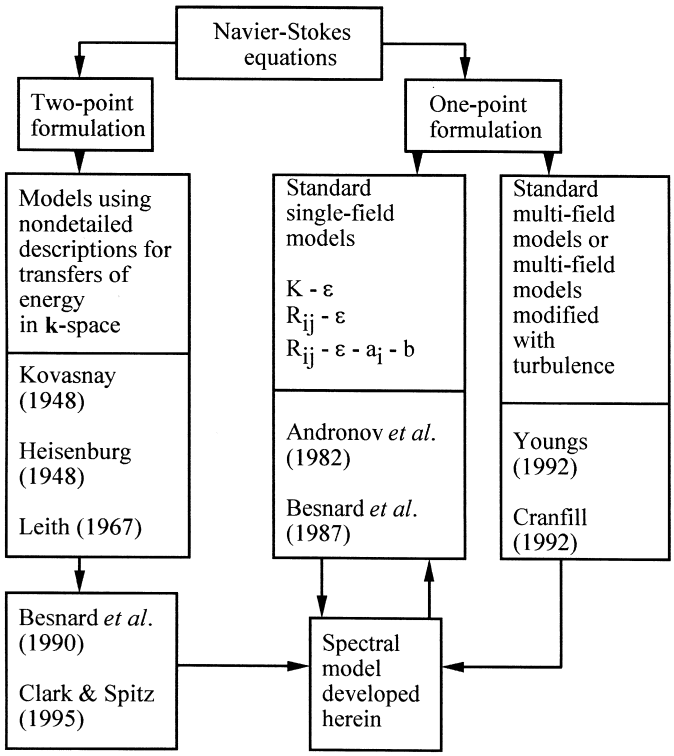

Fig. 1. Flow chart defining the ancestry of our spectral transport model.

interpenetration of two fluids. The Navier–Stokes equations are assumed to be relevant for both miscible and immiscible mixing.

At this stage of theoretical development, the attainment of a rigorous formulation, even for constant density flows, is not possible. During the last three decades of constant-density turbulence-transport developments, the model derivations have had to combine empiricism with rigor, and the same is true for the variable-density extensions. Constraints (dimensionality, preservation of conservation, tensor form, Galilean invariance, simplicity of form, and similar general considerations) serve to limit the choices for modeling. Comparisons with experiments likewise furnish guidance.

In this article we describe a spectral turbulence transport formulation for variable-density turbulence in circumstances of strong inhomogeneity and anisotropy. In Article II we show that moments of these equations introduce some auxiliary single-point variables. These are some of the elements that are missing from previous single-point formulations for variable-density turbulence (e.g. the BHR model).

The family of model-development work into which these variable-density turbulence activities fit is shown in the diagram of Fig. 1. The starting point for all directions is the Navier–Stokes equations.

Guidance for the spectral transport model developed herein is taken from the following three branches of transport modeling: the simple (local) closures describing transfers in k-space from the two-point branch (Besnard et al., 1996; Clark and Spitz, 1995), the single-point, single-fluid, turbulence transport models, and the single-point, two-field models. Another branch from the two-point box could be shown that handles the transfers of energy in k-space with much more detail, but no use is made of that approach for our model. Likewise other branches that exist are not shown since the ancestry of this model is composed of only these three branches.

Another branch that evolves from the Navier–Stokes equations leads to the two-field (or multifield) flow equations. Explicit modeling describes the principal interaction between discrete entities and fluid in terms of drag. Within the two-field formulation, the fluid interpenetration is described by terms in the equations that contain no contributions from fluctuations away from the mean within each field. This interpenetration, termed herein an 'ordered' process, is discussed by Steinkamp (1996). In addition, a 'disordered' component of the interpenetration can be expected to arise as a result of fluctuations away from the mean flow. The turbulence transport equations are capable of representing this 'disordered' component of interpenetration. The two-field equations are capable of exhibiting the origin for these fluctuations. They are unstable whenever there is relative motion between the two fluids. Thus the two-field formulations contain hints of a disordered component to interpenetrating flow but require further modeling for practical exploitation of this feature. As usually written, two-field models are incapable of representing crucial aspects of the general turbulent dynamics that we seek to describe.

Directly descendent from the two-field models are those that have been extended to include the missing processes; such as an evolving length scale, and turbulence. These modifications are derived through empirical and heuristic arguments and are discussed by Steinkamp et al. (1995).

2. The two-fluid spectral approach

For two or more interacting fluids, the usual approach to describing their interpenetration has been through the use of two-field or multifield equations, as described above. One might also consider the problem in terms of a single field of variables in which there are large variations in fluid density. Single-point models have been described, and applied with some success, by Andronov et al. (1982), Nikiforov (1991), and Besnard et al. (1992). Two-point models are only recently being investigated, notably by Clark and Spitz (1995), Godeferd and Cambon (1994) for homogeneous circumstances, Besnard et al. (1995) and this current work for inhomogeneous configurations.

In this study we obtain correlations that are functions of two points in space. We pass to wave-vector space by means of Fourier transforms with respect to the separation variable of the two points. For the sake of simplicity we angularly integrate these equations in (wave vector) **k**-space thus reducing the spectral dependence to (wave number) k. This transformation allows for an identification of length scales to Fourier modes. We realize that this simplification captures only the real part and not the imaginary part of the spectrum and that a significant portion of the physics involving directional dependence in Fourier space is averaged out of the equations. For now, however, we feel that a fully three-dimensional **k**-space model is unwarranted due to lack of any experimental data to verify such a model.

In the current form of our representations, we are not especially concerned with density discontinuities. For our purposes the dominant spectral structure is associated with relatively large clouds or blobs of a dispersed phase and with large-scale structures. Thus we ignore for now the behavior of the fine-scales, e.g. the dissipation range at high k.

Building on the work of Clark and Spitz (1995), we incorporate guidance from two-field formulations and from many of the constant-density developments, both single-point and spectral. These relationships are discussed more fully in the next section, which describes the equations and the origins of contributing terms.

We require mass, momentum, and energy conservation in both physical and wave-number space in the inviscid limit. Any candidate model terms must be of the proper tensor formulation, that is to say, they must have the same free indices, same symmetries, same invariants, and be dimensionally consistent with the unmodeled terms. We also demand that the model terms integrate (over wave numbers) to reasonable single-point forms. In the absence of further guidance, for candidate model terms we invoke simplicity, manifested by the omission of certain products of first derivatives and of higher than second derivatives (in the spirit of the Stokes stress tensor in the Navier–Stokes equations). These constraints lead to simple low-order approximations (e.g. for cascade in k-space) that capture much of what appears to be happening, as illustrated by the test examples described in Article II.

To summarize the motivations for developing a tractable and broadly applicable spectral formulation for turbulence in a fluid with variable density, we have mentioned its relationship to the enhancement of single-point models. In Section 1 we pointed out that a transport equation for the single-point dissipation tensor, ϵ_{ij}, must be derived. For this endeavor, the knowledge of the scales associated with the turbulence proves very useful for formulating credible ϵ_{ij} equations. A spectral formulation may also provide a basis on which to construct scale information of the turbulence.

The additional spectral information frees the modeling from the simplistic characterization of turbulence by the magnitude of turbulence kinetic energy (K) and a turbulent length scale (L), or a dissipation rate (ϵ), leading to less simplistic modeling assumptions. Unlike single-point models, the spectral formulation is not inherently limited to certain regimes of Reynolds numbers. Hence, spectral representations potentially allow a much greater scope of interesting problems to be solved realistically, albeit at greater computational expense, and allow the derivation of model equations that can go beyond one-point formulations in their applicability (as shown in Article II).

3. Formulation of the model equations

Development of the spectral model equations is described schematically in Fig. 2. From the spectral formulation there radiate numerous directions for investigation as shown in Fig. 3.

The physical processes described by our spectral transport equations are of three types, advective, pressure-related and viscous. For each there are several features that need representation. Advective processes strongly influence the kinematics of mixing. These

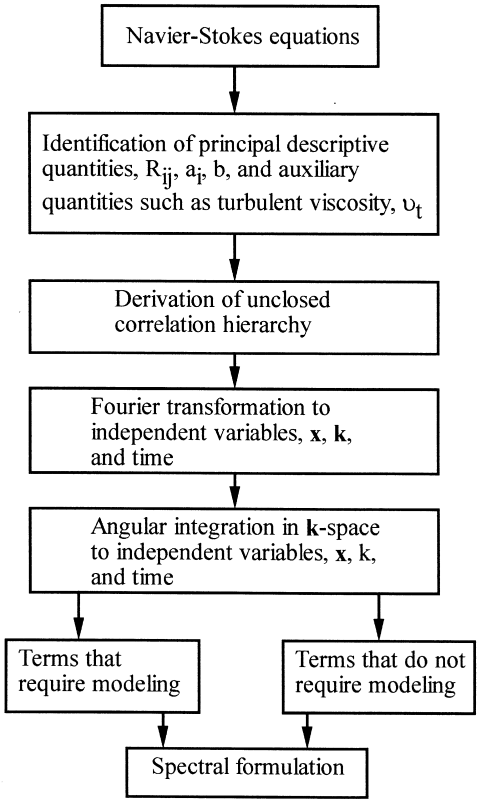

Fig. 2. Flow chart describing steps of the spectral formulation.

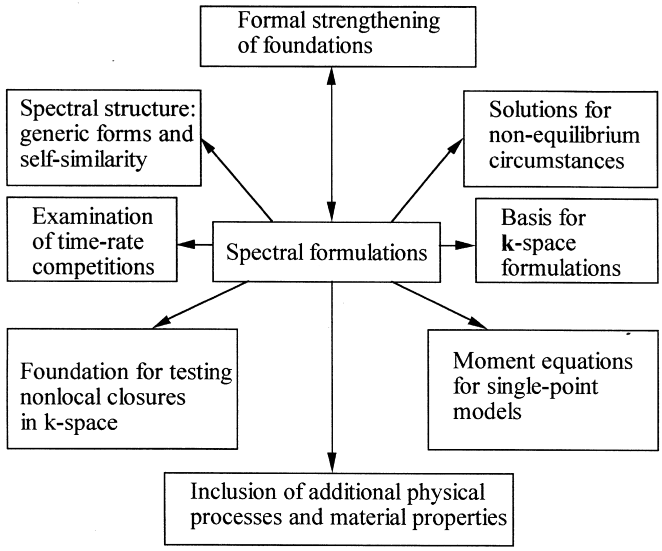

Fig. 3. Flow chart describing all of the potential uses of a spectral formulation.

processes are accounted for as both mean-flow and stochastic advective transport and serve as source terms in the Reynolds stress transport equation. Pressure is both a local and global process. Locally, pressure effects are manifested as differential acceleration and momentum exchange between fluid parcels of differing mass, the latter of which has historically been represented as drag. Nonlocally, pressure effects motivate mean-flow coupling and diffusion terms in physical space, as well as cascade and return to isotropy in wave number space.

4. The spectral equations

Following the usual convention of single-point turbulence modeling of variable density flows, the flow field variables, i.e. density, ρ, velocity, $\mathbf{u}$, and pressure, p, are decomposed into their mean and fluctuating parts and substituted into the conservation equations. The decompositions are

$$\rho = \bar{\rho} + \rho' \tag{1a}$$

$$\mathbf{u} = \bar{\mathbf{u}} + \mathbf{u}' \tag{1b}$$

$$p = \bar{p} + p' \tag{1c}$$

where the overbar denotes the uniformly weighted ensemble average and the prime denotes a fluctuation about the average with the average of a fluctuating quantity equal to zero. For variable density flows, it is useful to incorporate the mass-weighted averaging procedure introduced by Favre which leads to a conservative form of the Reynolds stress tensor, R_{ij}, in the averaged momentum equations, where $R_{ij} = \overline{\rho u_i'' u_j''}$. Thus the averaged mass-weighted velocity, $\tilde{\mathbf{u}}$, is defined as

$$\tilde{\mathbf{u}} = \frac{\overline{\rho \mathbf{u}}}{\bar{\rho}} \tag{2}$$

and $\mathbf{u}''$ denotes the mass-weighted fluctuation about this averaged quantity, such that $\mathbf{u} = \tilde{\mathbf{u}} + \mathbf{u}''$ with $\overline{\rho \mathbf{u}''} = 0$.

If we apply the Reynolds decomposition to this momentum density, $\overline{\rho \mathbf{u}}$, we get

$$\overline{\rho \mathbf{u}} = \overline{(\bar{\rho} + \rho')(\bar{\mathbf{u}} + \mathbf{u}')} = \overline{\rho}\,\overline{\mathbf{u}} + \overline{\rho' \mathbf{u}'} \tag{3}$$

In order to identify a velocity that corresponds to the mean mass flux, we can use the Favre mass-weighted velocity, $\tilde{\mathbf{u}}$. Thus we incorporate the mass-weighted velocity into the expression for momentum density to get

$$\tilde{\mathbf{u}} = \bar{\mathbf{u}} + \frac{\overline{\rho' \mathbf{u}'}}{\bar{\rho}} \tag{4}$$

We define another important variable here, namely the velocity $\mathbf{a}$, associated with the net turbulence mass flux relative to $\tilde{\mathbf{u}}$. From Eq. (4), it is apparent that this velocity associated with the mass flux is just

$$\mathbf{a} = \frac{\overline{\rho' \mathbf{u}'}}{\bar{\rho}} \tag{5}$$

The idea that this quantity describes the fluxing of mass relative to $\tilde{\mathbf{u}}$, is demonstrated by the resulting expression:

$$\tilde{\mathbf{u}} = \bar{\mathbf{u}} + \mathbf{a} \tag{6}$$

Due to the importance of this quantity, the model discussed herein transports this quantity, namely $\mathbf{a}$, which is derived from the Navier–Stokes equations. The transport equation for $\mathbf{a}$ contains a source term composed of the mean pressure gradient coupled to a kind of density correlation, b, where $b = -\overline{\rho'(1/\rho)'}$. A transport equation for b is derived from the conservation of mass equation.

For two arbitrary points in space, $\mathbf{x}_1$ and $\mathbf{x}_2$, the two-point generalization of single-point statistics as introduced by Clark and Spitz (1995) are (we omit the argument t for brevity)

$$R_{ij}(\mathbf{x}_1, \mathbf{x}_2) = \frac{1}{2}\overline{[\rho(\mathbf{x}_1) + \rho(\mathbf{x}_2)] u_i''(\mathbf{x}_1) u_j''(\mathbf{x}_2)} \tag{7}$$

$$a_i(\mathbf{x}_1, \mathbf{x}_2) = -\overline{u_i''(\mathbf{x}_1)\rho(\mathbf{x}_1)\nu(\mathbf{x}_2)} \tag{8}$$

$$b(\mathbf{x}_1, \mathbf{x}_2) = -\overline{\rho'(\mathbf{x}_1)\nu'(\mathbf{x}_2)} \tag{9}$$

where

$$\nu(\mathbf{x}) = \frac{1}{\rho(\mathbf{x})} \tag{10}$$

Note that there are other forms that could be used for these quantities, which also satisfy the

requirement of reducing to the single-point form as $\mathbf{x}_1$ approaches $\mathbf{x}_2$ and possess the desired symmetries, i.e. those possessed by the constant density Reynolds stress tensor.

The constraints on the Reynolds stress tensor, as required by Clark and Spitz (1995), are

1. $R_{ij}(\mathbf{x}_1, \mathbf{x}_2) = R_{ij}(\mathbf{x}_2, \mathbf{x}_1)$
2. As $|\mathbf{x}_1 - \mathbf{x}_2| \to \infty$, $R_{ij}(\mathbf{x}_1, \mathbf{x}_2) \to 0$
3. $R_{ij}(\mathbf{x}_1, \mathbf{x}_2)$ remain bounded as $|\mathbf{x}_1 - \mathbf{x}_2| \to 0$

There is no obvious constraint as to which choice is best except that whatever is chosen must be correctly transported by the Navier–Stokes equations. The choice is thus dictated more by properties of manipulative ease and transparency of interpretation. Let us define

$$\mathbf{x} \equiv \frac{1}{2}(\mathbf{x}_1 + \mathbf{x}_2) \tag{11}$$

and

$$\mathbf{r} \equiv \mathbf{x}_1 - \mathbf{x}_2 \tag{12}$$

and substitute into the transported variables. We have for the additional Fourier transformations

$$R_{ij}(\mathbf{x}, k) \equiv \int R_{ij}(\mathbf{x}, \mathbf{r}) \mathrm{e}^{-ik\cdot\mathbf{r}} \, \mathrm{d}\mathbf{r} \tag{13}$$

$$a_i(\mathbf{x}, k) \equiv \int a_i(\mathbf{x}, \mathbf{r}) \mathrm{e}^{-ik\cdot\mathbf{r}} \, \mathrm{d}\mathbf{r} \tag{14}$$

$$b(\mathbf{x}, k) \equiv \int b(\mathbf{x}, \mathbf{r}) \mathrm{e}^{-ik\cdot\mathbf{r}} \, \mathrm{d}\mathbf{r} \tag{15}$$

In this report, we work with variables and equations that have been angularly averaged in **k**-space:

$$R_{ij}(\mathbf{x}, k) = \int R_{ij}(\mathbf{x}, k) \frac{k^2 \, \mathrm{d}\Omega_k}{(2\pi)^3} \tag{16}$$

$$a_i(\mathbf{x}, k) = \int a_i(\mathbf{x}, k) \frac{k^2 \, \mathrm{d}\Omega_k}{(2\pi)^3} \tag{17}$$

and

$$b(\mathbf{x}, k) = \int b(\mathbf{x}, k) \frac{k^2 \, \mathrm{d}\Omega_k}{(2\pi)^3} \tag{18}$$

where $\mathrm{d}\Omega_k = \sin\theta \, \mathrm{d}\theta \, \mathrm{d}\phi$ for $0 \leqslant \theta \leqslant \pi$; $0 \leqslant \phi \leqslant 2\pi$. From these we can recover the single-point forms

$$R_{ij}(\mathbf{x}) = \int_0^\infty R_{ij}(\mathbf{x}, k)\,\mathrm{d}k \tag{19}$$

$$a_i(\mathbf{x}) = \int_0^\infty a_i(\mathbf{x}, k)\,\mathrm{d}k \tag{20}$$

and

$$b(\mathbf{x}) = \int_0^\infty b(\mathbf{x}, k)\,\mathrm{d}k \tag{21}$$

Clark and Spitz (1995) derive equations for a completely statistically homogeneous configuration. For the inhomogeneous free mixing layer, we describe the necessary minimum extensions that we have found to give agreement with experiments. Thus we consider the special case of a mixing layer of infinite extent in the x and z directions, so that ensemble averages vary only with normal direction, y, scalar wave number, k, and time. For this configuration, the ensemble averages are assumed to be equivalent to spatial averages over x–z planes. The fluid is confined by stationary boundaries far above and below the turbulent mixing zone (TMZ), such that there is nowhere any vertical volumetric flux (i.e. the flow is incompressible) and $\bar{\mathbf{u}}(y, t) = 0$, and $\tilde{\mathbf{u}}(y, t) = \mathbf{a}(y, t)$. Hereafter, we will use R_{ij}, a_i, and b to indicate the spectral quantities and we will explicitly show their respective arguments only for the case of representing their single-point forms, i.e. when they are functions of the normal direction y and time only. Whereas the density, ρ, velocity, $\mathbf{u}$, pressure, p, turbulent length scale, S, and the turbulent kinetic energy, K, will always be functions of the normal direction y and time only. The acceleration, $\mathbf{g}$, varies only with time for these discussions.

The appropriate equations for $\bar{\rho}$ and $\tilde{\mathbf{u}}$ remain the same as for the inviscid single-point formulation. The equations are presented here for one spatial dimension, with $\tilde{u_y}$ and $a_y(y, t)$ representing the y-component of the respective velocity vectors.

$$\frac{\partial \bar{\rho}}{\partial t} + \frac{\partial \bar{\rho}\tilde{u}_y}{\partial y} = 0 \tag{22}$$

$$\frac{\partial \bar{\rho}\tilde{u}_y}{\partial t} + \frac{\partial \bar{\rho}\tilde{u}_y\tilde{u}_y}{\partial y} = -\frac{\partial \bar{p}}{\partial y} - \frac{\partial R_{yy}}{\partial y} + \bar{\rho} g_y \tag{23}$$

$$\tilde{u}_y = a_y(y, t) \tag{24}$$

The new equations for the spectral variables, a_y, b, R_{nn} and R_{yy} are presented in the following discussion, along with descriptions of the R_{nn}-contributing terms in each. Assuming axisymmetry, so that $R_{xx} = R_{zz}$, the values for these quantities can be determined by knowing R_{yy} and R_{nn}. For this configuration in principal coordinates, R_{ij} has no off-diagonal components. With the addition of horizontal shear the additional Reynolds stress components are analogous to those presented by Besnard et al. (1996) in their analysis of a free shear, and equations for R_{xy} and/or R_{zy} are obtained as straightforward extensions.

For a_y, we write

$$\frac{\partial a_y}{\partial t} = -\tilde{u}_y \frac{\partial a_y}{\partial y} + \frac{b}{\bar{\rho}} \frac{\partial \bar{p}}{\partial y} - \left[C_{\mathrm{rp1}} k^2 \sqrt{a_n a_n} + C_{\mathrm{rp2}} k \sqrt{\frac{k R_{nn}}{\bar{\rho}}} \right] a_y - \frac{R_{yy}}{\bar{\rho}^2} \frac{\partial \bar{\rho}}{\partial y} + \frac{\partial}{\partial k} \left\{ k^2 \sqrt{\frac{k R_{nn}}{\bar{\rho}}} \left[-C_1 a_y + C_2 k \frac{\partial a_y}{\partial k} \right] \right\} + C_d \frac{\partial}{\partial y} \upsilon_t \frac{\partial a_y}{\partial y} \tag{25}$$

The contributing terms, discussed in the order they appear on the right side, are:

(1) The advective term

$$-\tilde{u}_y \frac{\partial a_y}{\partial y}$$

(2) A principal driving term

$$\frac{b}{\bar{\rho}} \frac{\partial \bar{p}}{\partial y}$$

written as a direct extension to the term in single-point formulation, on the assumption that spectral b produces spectral **a** at the same wave number. Direct numerical simulations (DNS) of Sandoval (1995) indicate that there are modifications to this term which arise from inclusion of appropriate modeling of the closure for a single-point term like

$$\bar{\rho} \overline{\left(\frac{1}{\rho} \right)' \frac{\partial p'}{\partial x_i}} \tag{26}$$

The effect can be described by using some appropriate fraction of b in this source term; we have not, however, included this modification in our present investigations. The assumption that b produces a_y at the same k may be justified by the fact that b couples directly to $\nabla \bar{p}$ to produce a_y, see Clark and Spitz (1995) for a discussion of the homogeneous case. Sandoval (1995) has also indicated that this is true from his DNS calculations of homogeneous variable density turbulence. Note that this term contributes a pressure gradient to the equation $\tilde{u}_y = a_y(y, t)$, which serves to determine the value of the pressure gradient at every time through the transient dynamics.

(3) The representation of drag between the two fluids is

$$-\left[C_{\mathrm{rp1}} k^2 \sqrt{a_n a_n} + C_{\mathrm{rp2}} k \sqrt{\frac{k R_{nn}}{\bar{\rho}}} \right] a_y$$

The C_{rp1} term represents the form drag C_{rp1} is directly related to the drag coefficient that Youngs (1992) found to be an order of magnitude greater than the classical value. In Article II we confirm the Youngs finding and attribute the necessity for large magnitude to the effects of convoluted flow paths along the interface between the fluids. The C_{rp2} term represents a 'viscous-like' drag, in this case resulting from effective turbulence viscosity rather than molecular viscosity. These two terms are derived directly as extensions of the usual two-field

formulation. There are some possible alternative expressions for these drag terms which could incorporate relevant effects that are nonlocal in wave number space. For example, we could consider replacing

$$-C_{\mathrm{rp1}}k^2\sqrt{a_n a_n} \tag{27}$$

by

$$-C_{\mathrm{rp1}}\int_0^{k_1} k\sqrt{a_n a_n}\,\mathrm{d}k \tag{28}$$

This nonlocal form describes contributions to drag at wave number k from all other wave numbers lying between $k = 0$ and $k = k_1$. There is no difficulty with this formulation if we attempt to let $k_1 \to \infty$. With the expectation that $a_y \to k^{-m}$, with $m > 2$, for large k (see form-function discussion in Appendix C), the integral converges in that limit. Similar comments can be made about possible nonlocal forms for the C_{rp2} term. It is tempting to consider various nonlocal drag expressions because of the heuristic idea that the effects of many wave numbers can combine collectively to transfer momentum at any particular wave number between the fluids. At this stage we have not found any formulation that works better than the simple local form, insofar as comparisons with experimental data are concerned. In addition, these terms could also depend in a nontrivial fashion on dimensionless functions of dimensionless $b(y, t)$.

(4) A second principal drive term is

$$-\frac{R_{yy}}{\bar{\rho}^2}\frac{\partial\bar{\rho}}{\partial y}$$

This term is called the gradient-flux term because whenever it is roughly balanced by drag, the result is an expression for $\bar{\rho}a_y$ (the spectral mass flux), proportional to the gradient of $\bar{\rho}$. Term 2, in contrast, can contribute a counter-gradient flux, notably when reversal of acceleration turns the mixing zone into a demixing zone. More generally, the two principal drive terms, 2 and 4, interact with the other terms in the a_y equation in various possible ways. In the start-up phase of unstable mixing, the pressure-gradient term acts wherever b is seeded at the interface to drive a strongly-ordered part of $\partial a_y/\partial t$. The growing value of a_y interacts with the pressure gradient in the R_{nn} and R_{yy} equations (see below), which produces a disordered component of Reynolds stress, giving in turn a source to a disordered component of $\partial a_y/\partial t$. In this mixing stage of the TMZ growth, the two sources reinforce each other. As the TMZ dynamics mature into self-similar growth, the large-wave-number components of b may cascade into an inactive range, which means that for those wave numbers the pressure-gradient source to $\partial a_y/\partial t$ has changed to essentially complete balance with the drag term. Only the low-wave-number parts of b (along with the density-gradient source) are effective in perpetuating the continuing self-similar growth of a_y. Thus the spectrum of b can be considered to possess an 'active' low-k part and a 'passive' high-k part. The partitioning of the spectrum into active and passive parts is significant for the development of one-point models. More details regarding this concept of active and passive parts of the b spectrum are given in Article II in the discussion of acceleration reversal. If the acceleration, **g**, suddenly vanishes, then only the no. 4 source term remains to continue widening the TMZ; however, its effectiveness for this purpose is

significantly curtailed by the drag (3) and cascade (5) terms. When **g** is completely reversed, there is an adjustment period in which the no. 2 source term works in concert with drag (3), across all parts (previously active and passive) of the b spectrum, to accomplish the reversal of a_y. This sequence of events represents a spectral nonequilibrium process. Only when a_y has changed sign do these terms again oppose each other and the passive part of the b spectrum return to dormancy. It is interesting to confirm in calculations of these processes that the passive part of the b spectrum indeed has very little effect on the overall spectrally integrated dynamics, as demonstrated in Article II by a comparison of two calculations, one that retains the passive part and the other that discards it. The only significant difference between the two calculations lies in the value of b; everything else is essentially the same.

(5) The cascade terms are

$$\frac{\partial}{\partial k}\left\{k^2\sqrt{\frac{kR_{nn}}{\bar{\rho}}}\left[-C_1 a_y + C_2 k\frac{\partial a_y}{\partial k}\right]\right\}$$

These are both conservative in k-space. They are based on the model proposed by Leith (1967) for local cascade, with a wave-like part (the C_1 term) and a diffusive part (the C_2 term); see Besnard et al. (1996) for an extensive discussion. With $C_1 > 0$ the wave-like cascade is forward (i.e. to higher wave numbers). Of necessity, $C_2 > 0$, resulting in both forward and reverse contributions to cascade. Several nonlocal forms of cascade representation have been considered. These nonlocal forms attempt to represent the triad interactions associated with triple-correlation terms in the formal derivation for constant-density turbulence as integrals over k-space (e.g. EDQNM (Orszag, 1970) or DIA (Kraichnan, 1958, 1959, 1964, 1965) derivations). Integral formulations for the variable density case are not yet rigorously developed, but one way to accomplish some degree of nonlocality would come (as in the drag term 3) from replacement of the local cascade rates by nonlocal integral cascade rates, for example

$$k\sqrt{\frac{kR_{nn}}{\bar{\rho}}} \tag{29}$$

becomes

$$\sqrt{\int_0^{k_1} k^2\frac{R_{nn}}{\bar{\rho}}\,\mathrm{d}k} \tag{30}$$

Both forms are essentially equivalent in the inertial range. It should be noted that R_{nn} is not necessarily a nonnegative definite function; hence the simpler local form of Eq. (29) will fail for circumstances of $R_{nn} < 0$. Clark and Spitz (1995) chose the form in Eq. (30) on this basis and also on the observation that the so-called 'catastrophe time' (Lesieur, 1990) for constant-density isotropic turbulence is predicted with somewhat better agreement to EDQNM, and for its ability to reproduce the so-called k^{-1} 'Batchelor scaling'. However, for most circumstances, we have seen little difference between the results using either cascade rate time-scale, and we have not encountered negative values of R_{nn}; thus we have opted for the simpler form of

Eq. (29). Indeed, it appears, as stated above, that the modeling constraints (conservation, tensor form, dimensionality, etc.) used for our cascade (and other) terms enable the simplest forms (like term 5) to capture much of the relevant physical processes.

It should be noted that cascade rates proportional to $k^2\sqrt{ka_n(y,t)a_n(y,t)}$ may be proposed on dimensional grounds (Clark and Spitz, 1995), although their physical significance is not obvious and their inclusion in calculations produces very minor effects, neither helpful nor harmful in matching results with existing experimental data. Similar to the discussion of no. 5 for the a_y equation, this expression is not a nonnegative definite function, and a similar argument is used for our choice of cascade rates.

(6) Spatial diffusion,

$$C_{\mathrm{d}}\frac{\partial}{\partial y}\upsilon_{\mathrm{t}}\frac{\partial a_y}{\partial y}$$

This term, which is intended to represent the action of the triple correlations as well as the pressure velocity correlations, is the same as used by many previous authors and requires two comments pertaining to the possible choices for expressions for the turbulent viscosity, υ_{t}: first, it is well known that the eddy viscosity, υ_{t}, should be modeled nonlocally; and second, the processes associated with an eddy viscosity are anisotropic. Nevertheless, until further investigation, for simplicity we chose the isotropic form

$$\upsilon_{\mathrm{t}} = \int_0^\infty \sqrt{\frac{kR_{nn}}{\bar{\rho}}}\frac{\mathrm{d}k}{k^2} \tag{31}$$

which reduces to the commonly used single point form

$$\upsilon_{\mathrm{t}} = 0.09S\sqrt{K} \tag{32}$$

in which S is the mean turbulent length scale and K is the total turbulence energy per unit mass. To accomplish this correspondence, an identification of a generic form function for R_{nn} in k-space and the performance of an appropriate moment integral, as discussed in Article II is required. An appropriate C_{d} must also be chosen.

Next, for b we write

$$\frac{\partial b}{\partial t} = \left(\frac{2\bar{\rho}-\rho_1-\rho_2}{\rho_1\rho_2}\right)\frac{\partial \bar{\rho}a_y}{\partial y} - C_{\mathrm{fb}}\left[\bar{\nu}^2\frac{\partial}{\partial y}\left(\frac{\bar{\rho}}{\bar{\nu}}\right)\right]\frac{\partial ka_y}{\partial k} + \frac{\partial}{\partial k}\left\{k^2\sqrt{\frac{kR_{nn}}{\bar{\rho}}}\left[-C_1 b + C_2 k\frac{\partial b}{\partial k}\right]\right\} + C_{\mathrm{d}}\frac{\partial}{\partial y}\upsilon_{\mathrm{t}}\frac{\partial b}{\partial y} - C_{\mathrm{db}}k^2 Db \tag{33}$$

The contributing terms on the right side are:

(1) The kinematical source term,

$$\left(\frac{2\bar{\rho}-\rho_1-\rho_2}{\rho_1\rho_2}\right)\frac{\partial \bar{\rho}a_y}{\partial y}$$

derived by Steinkamp (1996) for single-point transport of b. Because this term describes the effects of fluid mass transfer, there is no requirement for an advective term in the b equation. This term maintains the value of b at nearly its configurational value, namely $\theta_1\theta_2(\rho_1-\rho_2)^2/\rho_1\rho_2$ (Besnard et al., 1992), where θ_1 and θ_2 are the volume fractions of fluid 1 and fluid 2, respectively.

(2) The transport of b through wave-number space,

$$-C_{\mathrm{fb}}\left[\bar{\nu}^2\frac{\partial}{\partial y}\left(\frac{\bar{\rho}}{\bar{\nu}}\right)\right]\frac{\partial k a_y}{\partial k}$$

as induced by the presence of inhomogeneity in the mixture of fluids. This term is formally derived as a next-higher-order contribution to the Taylor expansion of points, $\mathbf{x}_1$ and $\mathbf{x}_2$ about the central point, $\mathbf{x}$. It resembles the C_{f} terms previously proposed by Besnard et al. (1996) which describe the mean-flow-shear-induced distortions of turbulence spectra in a constant-density fluid. In that case, the term contributes to the vortex-pairing process that occurs in a free shear layer. Here it contributes to the bubble-amalgamation process that is known to occur in the self-similar stages of TMZ growth at small wave numbers and to an alteration of cascade that occurs through 'eddy distortion' at high wave numbers. Its presence is crucial to the achievement of agreement with experiments. A higher-order degree of nonlocality (e.g. an integral expression) may be appropriate, but at this stage there is no proof of the necessity for this complication.

A heuristic derivation of this term suggests that it must couple the inhomogeneity as described by $\nabla\bar{p}/\bar{\rho}$, with the presence of mass interpenetration, described by a_y. (Direct coupling to $\nabla\bar{p}/\bar{\rho}$ seems implausible, as this contributes to the creation of interpenetration and is not a measure of its current level.) Dimensional arguments restrict the possibilities appreciably; adding the necessity for conservation in k-space leads to a form proportional to

$$\frac{1}{\bar{\rho}}\frac{\partial\bar{\rho}}{\partial y}\frac{\partial k a_y}{\partial k} \tag{34}$$

which is very close to the form that arises in the two-point advection terms, as derived in Appendix B.

(3) The cascade terms,

$$\frac{\partial}{\partial k}\left\{k^2\sqrt{\frac{kR_{nn}}{\bar{\rho}}}\left[-C_1 b + C_2 k\frac{\partial b}{\partial k}\right]\right\}$$

These have the same form as the cascade terms for a_y, and the same comments apply here.

(4) The spatial diffusion term,

$$C_{\mathrm{d}}\frac{\partial}{\partial y}\upsilon_{\mathrm{t}}\frac{\partial b}{\partial y}$$

(5) The decay term resulting from molecular diffusion between species,

$$-C_{\mathrm{db}}k^2 Db$$

for which the kinematic diffusion coefficient is D. In this work, $D \to 0$.

Next, for R_{nn} and R_{yy} we write

$$\frac{\partial R_{nn}}{\partial t} = -\frac{\partial R_{nn}\tilde{u}_y}{\partial y} + \int_{-\infty}^{+\infty}\left(2a_y\frac{\partial \bar{p}}{\partial y}\right)(k\exp(-2k \mid y' - y \mid))\,\mathrm{d}y' - 2R_{yy}\frac{\partial \tilde{u}_y}{\partial y} + C_{\mathrm{d}}\frac{\partial}{\partial y}\upsilon_{\mathrm{t}}\frac{\partial R_{nn}}{\partial y} + \frac{\partial}{\partial k}\left\{k^2\sqrt{\frac{kR_{nn}}{\bar{\rho}}}\left[-C_1 R_{nn} + C_2 k\frac{\partial R_{nn}}{\partial k}\right]\right\} \tag{35}$$

and

$$\frac{\partial R_{yy}}{\partial t} = -\frac{\partial R_{yy}\tilde{u}_y}{\partial y} + \int_{-\infty}^{+\infty}\left(2a_y\frac{\partial \bar{p}}{\partial y}\right)(k\exp(-2k \mid y' - y \mid))\,\mathrm{d}y' - 2R_{yy}\frac{\partial \tilde{u}_y}{\partial y} + C_{\mathrm{d}}\frac{\partial}{\partial y}\upsilon_{\mathrm{t}}\frac{\partial R_{yy}}{\partial y} + \frac{\partial}{\partial k}\left\{k^2\sqrt{\frac{kR_{nn}}{\bar{\rho}}}\left[-C_1 R_{yy} + C_2 k\frac{\partial R_{yy}}{\partial k}\right]\right\} + C_{\mathrm{m}}\int_0^k \sqrt{\frac{kR_{nn}}{\bar{\rho}}}\,\mathrm{d}k\left(\frac{1}{3}R_{nn} - R_{yy}\right) \tag{36}$$

The contributing terms on the right side are:

(1) The advective term,

$$-\frac{\partial R_{ij}\tilde{u}_n}{\partial x_n}$$

In contrast to the a_y equation, in which the conservation of mass equation is used to remove $\bar{\rho}$ from

$$\frac{\partial \bar{\rho}a_y}{\partial t} + \frac{\partial \bar{\rho}a_y\tilde{u}_y}{\partial y} = \ldots \tag{37}$$

these similar terms in the equations for R_{ij} retain the $\bar{\rho}$ that is intrinsically present in the generalized expression for the Reynolds stress (Eq. (7)).

(2) A principal driving term,

$$\int_{-\infty}^{+\infty}\left(2a_y\frac{\partial \bar{\rho}}{\partial y}\right)(k\exp(-2k \mid y' - y \mid))\,\mathrm{d}y'$$

coupling a_y with the mean pressure gradient. This process is intrinsically nonlocal in physical space, with effects that reach progressively farther away for wave numbers approaching zero (i.e. for large scales). The basis for this nonlocality lies in the propagation of pressure waves. In linear Kelvin–Helmholtz or Rayleigh–Taylor stability analysis the effects are manifested in a

velocity potential that varies as $\exp[-k|y|]$, where $|y|$ is the distance from the center of the instability layer. Thus the spreading of R_{ij}, which varies as the square of velocity fluctuations, is represented by the factor $\exp[-2k|y|]$, as shown in this term. Otherwise the coupling of a_y with the pressure gradient is the same as the single-point coupling. The basis and consequences of this nonlocality in physical space are discussed further in Appendix A.

(3) Another principal driving term,

$$-R_{in}\frac{\partial \tilde{u}_i}{\partial x_n} - R_{jn}\frac{\partial \tilde{u}_i}{\partial x_n}$$

coupling R_{yy} to gradients of $\tilde{u}_y$. This standard term (Besnard et al., 1996) is well known, especially for constant-density turbulent flows, but it is equally relevant here (although of relatively minor importance for the TMZ studies).

(4) The spatial diffusion term,

$$C_{\mathrm{d}}\frac{\partial}{\partial x_n}\upsilon_{\mathrm{t}}\frac{\partial R_{ij}}{\partial x_n}$$

As in the a_y and b equations, the form to be used can be local or any of several nonlocal variants.

(5) The cascade terms,

$$\frac{\partial}{\partial k}\left\{k^2\sqrt{\frac{kR_{nn}}{\bar{\rho}}}\left[-C_1 R_{ij} + C_2 k\frac{\partial R_{ij}}{\partial k}\right]\right\}$$

The same formulation and comments apply here as for the cascade of a_y.

(6) The return-to-isotropy term,

$$C_{\mathrm{m}}\int_0^k \sqrt{\frac{kR_{nn}}{\bar{\rho}}}\,\mathrm{d}k\left(\frac{1}{3}R_{nn} - R_{ij}\right)$$

which appears only in the deviatoric components of R_{ij}. The return rate can be written either in local form or, as shown, in the nonlocal form

$$C_{\mathrm{m}}\int_0^k \sqrt{\frac{k'R_{nn}}{\bar{\rho}}}\,\mathrm{d}k' \tag{38}$$

Another possible nonlocal form addresses the issues discussed in term 5 of the a_y equation and can be written as:

$$C_{\mathrm{m}}\sqrt{\int_0^k (k')^2\frac{R_{nn}}{\bar{\rho}}\,\mathrm{d}k'} \tag{39}$$

We have tried both forms for the return-to-isotropy rate and have found negligible difference.

A discussion on the choice of values for the model coefficients is given in Article II. For reference, we present those model coefficients here and we also give the generalized Cartesian tensor form of our base-model equations using the local form of the pressure gradient source term in the Reynolds stress transport equation instead of the nonlocal form. The reason for this is that we have not yet tested a nonlocal form of the source term for a completely general mixing circumstance. In the reference frame with $\bar{u}_y \equiv 0$,

$$\frac{\partial a_i}{\partial t} = -\tilde{u}_n \frac{\partial a_i}{\partial x_n} + \frac{b}{\bar{\rho}} \frac{\partial \bar{p}}{\partial x_i} - \left[C_{\mathrm{rp1}} k^2 \sqrt{a_n a_n} + C_{\mathrm{rp2}} k \sqrt{\frac{k R_{nn}}{\bar{\rho}}} \right] a_i - \frac{R_{in}}{\bar{\rho}^2} \frac{\partial \bar{\rho}}{\partial x_n}$$

$$+ \frac{\partial}{\partial k} \left\{ k^2 \sqrt{\frac{k R_{nn}}{\bar{\rho}}} \left[-C_1 a_i + C_2 k \frac{\partial a_i}{\partial k} \right] \right\} + \frac{C_{\mathrm{d}}}{\bar{\rho}} \frac{\partial}{\partial x_n} \upsilon_{\mathrm{t}} \bar{\rho} \frac{\partial a_i}{\partial x_n} \tag{40}$$

$$\frac{\partial b}{\partial t} = \left(\frac{2\bar{\rho} - \rho_1 - \rho_2}{\rho_1 \rho_2} \right) \frac{\partial \bar{\rho} a_n}{\partial x_n} - C_{\mathrm{fb}} \left[\bar{\nu}^2 \frac{\partial}{\partial x_n} \left(\frac{\bar{\rho}}{\bar{\nu}} \right) \right] \frac{\partial k a_n}{\partial k}$$

$$+ \frac{\partial}{\partial k} \left\{ k^2 \sqrt{\frac{k R_{nn}}{\bar{\rho}}} \left[-C_1 b + C_2 k \frac{\partial b}{\partial k} \right] \right\} + C_{\mathrm{d}} \frac{\partial}{\partial x_n} \upsilon_{\mathrm{t}} \frac{\partial b}{\partial x_n} \tag{41}$$

$$\frac{\partial R_{ij}}{\partial t} = -\frac{\partial R_{ij} \tilde{u}_n}{\partial x_n} + a_i \frac{\partial \bar{p}}{\partial x_j} + a_j \frac{\partial \bar{p}}{\partial x_i} - R_{in} \frac{\partial \tilde{u}_j}{\partial x_n} - R_{jn} \frac{\partial \tilde{u}_i}{\partial x_n} + \frac{\partial}{\partial k} \left\{ k^2 \sqrt{\frac{k R_{nn}}{\bar{\rho}}} \left[-C_1 R_{ij} + C_2 k \frac{\partial R_{ij}}{\partial k} \right] \right\}$$

$$+ C_m \int_0^k \sqrt{\frac{k R_{nn}}{\bar{\rho}}} \, \mathrm{d}k \left(\frac{\delta_{ij}}{3} R_{nn} - R_{ij} \right) + C_{\mathrm{d}} \frac{\partial}{\partial x_n} \upsilon_{\mathrm{t}} \frac{\partial R_{ij}}{\partial x_n} \tag{42}$$

where the model coefficients have been set to:

$C_{\mathrm{rp1}} = 5.0$, $C_{\mathrm{rp2}} = 6.0$, $C_1 = 0.1212$, $C_2 = 0.0606$, $C_{\mathrm{d}} = 0.03$, $C_{\mathrm{fb}} = 0.5$, and $C_{\mathrm{m}} = 1.0$.

5. Conclusions

Clark and Spitz (1995) derive the exact unclosed two-point transport equations for the primary mass-averaged variables of our spectral model directly from the Navier–Stokes equations. The transport equations have been Fourier transformed with respect to the separation vector between the two points. Due to their complicated nature, the transport equations are angularly integrated in **k**-space to reduce the transport models to a simpler form in wavenumber k-space. This reduction is justified by the fact that the k-space captures a great deal of the phenomena of interest and is much less computer intensive than the fully three-dimensional **k**-space model. These derivations are given by Clark and Spitz (1995). Constraints and guidelines have been identified and incorporated for modeling the necessary closures for this variable density inhomogeneous model in k-space.

Three major enhancements of this spectral model over any single-point model are: (1) the alleviation of the need for a transport equation for the length scales of the transported turbulence variables; (2) the alleviation of the assumption of spectral equilibrium (a requirement for the validity of single-point model equations); and (3) a global representation of instantaneous pressure-wave propagation. The second of these two enhancements enables a spectral model to describe transient flows that are out of spectral equilibrium, whereas a single-point model cannot. Thus, with a spectral model we are able to correlate the concept of turbulence decay with the cascade of energy from large turbulent scales down to smaller scales defined by a transfer rate that may vary with time, space and scale size.

Acknowledgements

We are indebted to Rick Rauenzahn, Didier Besnard, and Murray Rudman for their insightful conversations over the past few years that have served to nurture the formulation of this work. Contributions from Roy Axford, Lance Collins, Rodman Linn, Mat Maltrud, Donald Sandoval, and Charles Zemach have also proved valuable to this work and are much appreciated. We are also grateful to Margaret Findley of the Fluid Dynamics Group for helping to design and prepare this manuscript. This work was performed at Los Alamos National Laboratory, which is operated by the University of California under the auspices of the United States Department of Energy (contract W-7405-ENG-36).

Appendix A

A.1. Nonlocal processes in physical space

Integral formulations in physical space enable the characterization of instantaneous pressure-wave propagation of fluctuations from one point in physical space to another. Thus, for example, the existence of mean-flow shear can contribute to the nonlocal creation of turbulence at localities lying outside the shear layer. Likewise a TMZ between two fluids, subjected to a mean-field pressure gradient, can manifest the effects of differential acceleration beyond the borders of the mixing zone.

Classical Rayleigh–Taylor analysis for the linear instability of an interface introduces a velocity potential that varies as $\exp(-k|y|)$, in which $|y|$ is the distance from the interface (Chandrasekhar, 1961). If we assume that the amplitude of the perturbation on the interface is approximately half the width of the TMZ, then for a TMZ with width W and for wave numbers such that $kW > 1.0$, the linear theory does not apply. For parts of the turbulence spectrum with $kW \ll 1.0$, however, the linear theory is relevant and shows that fluctuating components of velocity extend appreciably beyond the boundaries of the TMZ. This nonlocal production of velocity fluctuations translates into a nonlocal source for R_{ij}. It does not, however, indicate nonlocal sources for a_y or b, which are associated with the transport of fluid

rather than pressure effects. Therefore we do not use nonlocal sources for a_y or b. For b, there are no pressure terms to provide this effect; for a_y, preliminary simulations of Sandoval (1995) indicate fluctuating pressure correlations act to modify the $b\nabla\bar{p}$, which is already included as a local term.

Guided by the results of linear analysis, we thus have modified the source terms for R_{nn} and R_{yy} in the following manner. The local form,

$$\frac{\partial R_{nn}}{\partial t} = 2a_y \frac{\partial \bar{p}}{\partial y} \tag{A1}$$

is rewritten

$$\frac{\partial R_{nn}}{\partial t} = \int_{-\infty}^{+\infty} \left[2a_y \frac{\partial \bar{p}}{\partial y} \right] Q(y', y)\, \mathrm{d}y' \tag{A2}$$

and similarly for R_{yy}.

The kernel $Q(y', y)$, 'nonlocality function,' must satisfy the condition

$$\int_{-\infty}^{+\infty} Q(y', y)\, \mathrm{d}y' = 1 \tag{A3}$$

For our problem we also expect it to depend only on $|y' - y|$ and to decrease as $\exp[-2k|y' - y|]$ as the separation between points increases. For large values of k, $Q(y', y)$ approaches a delta function. For now, we choose

$$Q(y', y) = k \exp[-2k \mid y' - y \mid] \tag{A4}$$

which satisfies the normalization condition, behaves in the required manner as $k \to 0$, and has the desired delta-function behavior as $k \to \infty$. It remains to be demonstrated, however, and we will now show that this 'spreading' factor allows the turbulence model to recover the linear Rayleigh–Taylor behavior as $k \to 0$. We will assume that the configuration starts at rest with only b present; the lowest order contribution to the evolution of a_y and R_{yy} (when both are still very small) is described by the following subset of Eqs. (25) and (35).

Consider the following parts at first without the $Q(y', y)$:

$$\frac{\partial R_{yy}}{\partial t} = 2a_y \frac{\partial \bar{p}}{\partial y} \tag{A5}$$

$$\frac{\partial a_y}{\partial t} = \frac{b}{\bar{\rho}} \frac{\partial \bar{p}}{\partial y} - \frac{R_{yy}}{\bar{\rho}^2} \frac{\partial \bar{\rho}}{\partial y} \tag{A6}$$

Differentiate the R_{yy} equation with respect to time, allowing only for the variation of a_y, and insert $\partial a_y/\partial t$ from the second equation.

$$\frac{\partial^2 R_{yy}}{\partial t^2} = -\frac{2}{\bar{\rho}^2}\frac{\partial \bar{p}}{\partial y}\frac{\partial \bar{\rho}}{\partial y}R_{yy} + \frac{2b}{\bar{\rho}}\left(\frac{\partial \bar{p}}{\partial y}\right)^2 \tag{A7}$$

The second term on the right, in the qualitative fashion of the other terms here omitted, is not relevant to this discussion, whereas the first term on the right contributes either an oscillatory component (if $\nabla\bar{p}(\nabla\bar{\rho}) > 0$) or an exponentially growing component (if $\nabla\bar{p}(\nabla\bar{\rho}) < 0$). This would appear to be the classic linear Rayleigh–Taylor solution but fails in that regard in one crucial respect.

To demonstrate this failure and its remediation, we note that, as it is written in local form, the first term distributes the turbulence energy only within the mixing layer itself. In that region for the unstable case, R_{yy} grows as

$$R_{yy} = R_{yy}(t=0)\exp[t\sqrt{2 \mid \nabla\bar{p}(\nabla\bar{\rho}) \mid /\bar{\rho}^2}] \tag{A8}$$

or

$$R_{yy} = R_{yy}(t=0)\exp[t\sqrt{2 \mid \Delta\rho g/\bar{\rho} \mid /W}] \tag{A9}$$

Where g is the y-component of $\nabla\bar{p}/\bar{\rho}$ and $\nabla\bar{\rho} = \Delta\rho/W$, with $\Delta\rho$ being the overall density difference across the TMZ of width W. In contrast, for an infinitesimal velocity squared, classic linear Rayleigh–Taylor analysis gives (Chandrasekhar, 1961)

$$R_{yy} = R_{yy}(t=0)\exp[2t\sqrt{k \mid \Delta\rho g \mid /2\bar{\rho}}] \tag{A10}$$

(Note the factor of 2, to describe growth of velocity-squared.) The essential difference between these two results is the occurrence of $1/W$ in the first and k in the second. In both cases, $R_{yy}(t=0)$ may depend on k, but the turbulence-transport result is essentially independent of k in the exponent. The reason, of course, is that the creation of R_{yy} in the purely local formulation confines the inertial resistance to growth to the mass within the mixing layer itself. In reality, as described above, the mass that must be set in motion extends well beyond the edges, so that R_{yy} can be expected to grow with a much reduced exponent for structures that are large compared to W, i.e. for $kW \ll 1$. Thus this local formulation preserves the spectral structure of $R_{yy}(t=0)$.

With nonlocality of $Q(y', y)$, the turbulence-transport results account for the added inertia and give the classical exponential growth. As a practical consequence, the behavior of TMZ growth and appearance is significantly altered; as a conceptual consequence, the influence of low wave numbers on self-similarity is quite different from that of the purely local theory. The nonlocal formulation does not preserve the spectral structure of $R_{yy}(t=0)$.

To demonstrate the remedial effects of including the nonlocal pressure-wave propagation, we return to the equation for R_{yy}, Eq. (A5), which is rewritten as follows:

$$\frac{\partial R_{yy}}{\partial t} = \int_{-\infty}^{+\infty} S_{yy}(y')k\exp[-2k \mid y' - y \mid]\,\mathrm{d}y' \tag{A11}$$

where

$$S_{yy}(y) \equiv 2a_y \frac{\partial \bar{p}}{\partial y} \tag{A12}$$

To isolate the essence of our demonstration, it is sufficient to consider, for $y > W/2$, the approximation (an overestimation by choosing S_{yy} at $y = 0$)

$$\frac{\partial R_{yy}}{\partial t} = \int_{-w/2}^{w/2} S_{yy}(y=0) k \exp[-2k \mid y' - y \mid] \, \mathrm{d}y'$$

$$= (S_{yy}(y=0)/2) \exp[-2ky](\exp(kW) - \exp(-kW)) \tag{A13}$$

Twice the integral over y', for $W/2 \leqslant y' < \infty$, thus gives the total amount of R_{yy} created per unit time outside of the TMZ, which accordingly is

$$\frac{\partial}{\partial t} R_{yy}(\text{outside}) = (S_{yy}(y=0)/k)[1 - \exp(-2kW)] \tag{A14}$$

The total amount created per unit time everywhere is (because of the normalization of Q) the same as the total amount due to the local-theory, namely $S_{yy}(y=0)W$. Thus the nonlocal prediction for total R_{yy} created inside the layer per unit time is

$$\frac{\partial}{\partial t} R_{yy}(\text{inside}) = S_{yy}(y=0) W \left[1 - \frac{1 - \exp(-2kW)}{2kW}\right] \tag{A15}$$

For $kW < 1$, we expand the exponent to get

$$\frac{\partial}{\partial t} R_{yy}(\text{inside}) \approx S_{yy}(y=0) k W^2 \tag{A16}$$

Divide this by W to get, within the layer,

$$\frac{\partial R_{yy}}{\partial t} = 2a_y(kW) \frac{\partial \bar{p}}{\partial y} \tag{A17}$$

With this alteration the exponential growth for kW small becomes

$$R_{yy} = R_{yy}(t=0) \exp[t\sqrt{2k \mid \Delta \rho g \mid / \bar{\rho}}] \tag{A18}$$

which now contains the essential dependence on k as seen in the solution to the classic linear Rayleigh–Taylor analysis, Eq. (A10).

It is interesting to contrast our approach to nonlocal pressure-wave effects with the technique employed by Demuren et al. (1994). They describe a procedure for 'local diffusion sources to be distributed over lengths of the order of the integral scale.' They implement this technique into a nonspectral transport model and report that it 'enabled the well-known free-stream edge singularity problem to be eliminated.' To the extent that turbulence self-diffusion receives contributions from the nonlocal triple-correlation terms that arise from pressure-velocity correlations through Greens-function integral solutions, we agree that turbulence

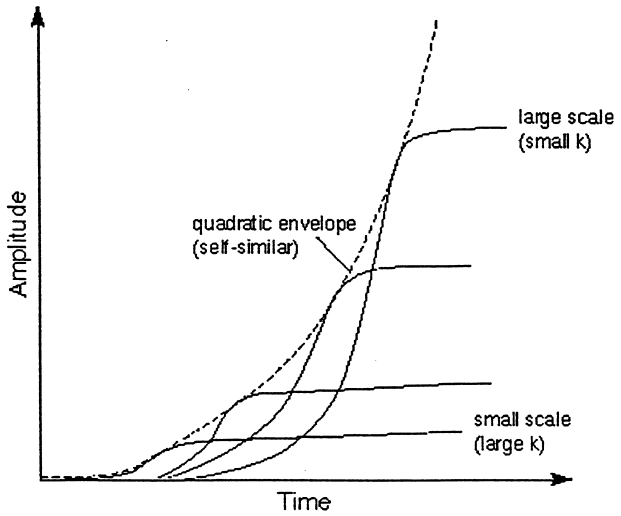

Fig. 4. Schematic to demonstrate the growth and saturation of initial perturbations of the Rayleigh–Taylor instability.

diffusion should be distributed nonlocally. This effect is physically visualized in a two-point (spectral) formulation of the theory. To capture the effects of inertial response on the creation of turbulence (and thus the Rayleigh-Taylor linear growth rate), we believe the principal nonlocal effect must be as described by our $Q(y', y)$ modification to the differential-acceleration term (and to the mean-flow shear coupling).

It is of interest to note the relation between this linear Rayleigh–Taylor analysis and the self-similar analysis for the turbulence equations described in Article II. If there is a rich spectrum of modes at $t = 0$, then each will grow exponentially, then saturate, creating an envelope for net growth of the fully nonlinear evolution (see Fig. 4).

This envelope has the quadratic behavior dictated by the dimensionality of acceleration, g. A heuristic analysis of this process starts with the linear growth equation for amplitude, A, at wave number k, and the density ratio, $(\rho_2-\rho_1)/(\rho_2+\rho_1)$,

$$\frac{\mathrm{d}^2A}{\mathrm{d}t^2}=\frac{kg(\rho_2-\rho_1)A}{(\rho_1+\rho_2)} \tag{A19}$$

and replaces k by $1/S$, where S is the currently dominant scale at which growth is occurring. With self-similarity, S is a fixed multiple of A; that is, $S = \beta A$. Then

$$\frac{\mathrm{d}^2A}{\mathrm{d}t^2}=\frac{g(\rho_2-\rho_1)}{\beta(\rho_1+\rho_2)} \tag{A20}$$

and

$$A = \frac{gt^2(\rho_2 - \rho_1)}{2\beta(\rho_1 + \rho_2)} \tag{A21}$$

If mode saturation were to occur when the magnitude of A is approximately 20% of S, then we get $A = [0.1(\rho_2 - \rho_1)/(\rho_1 + \rho_2)]^* gt^2$, which is consistent with the actually observed self-similar behavior of a TMZ, for which experiments give a coefficient of about 0.12.

Appendix B

B.1. Derivation of the advective-like term in the b-equation

The term in the b-equation which couples the gradients in the spectrum of a_i to the gradients in configuration space of ρ can be derived by consideration of a particular advective-like term arising in an exact b-equation. Consider terms of the following type (arguments are included here for additional clarity):

$$\frac{\mathrm{D}b(\mathbf{x}_1, \mathbf{x}_2)}{\mathrm{D}t} = -\bar{\nu}(\mathbf{x}_2)\frac{\partial\overline{\rho'(\mathbf{x}_1)u_n''(\mathbf{x}_2)}}{\partial x_{2n}} + \{\text{other terms}\} \tag{B1}$$

Clark and Spitz (1995) proposed the following model:

$$\overline{\rho'(\mathbf{x}_1)u_i''(\mathbf{x}_2)} = \bar{\rho}(\mathbf{x}_1)a_i(\mathbf{x}_1, \mathbf{x}_2) \tag{B2}$$

so

$$\frac{\mathrm{D}b(\mathbf{x}_1, \mathbf{x}_2)}{\mathrm{D}t} = -\bar{\nu}(\mathbf{x}_2)\frac{\partial\bar{\rho}(\mathbf{x}_1)a_n(\mathbf{x}_1, \mathbf{x}_2)}{\partial x_{2n}} + \{\text{other terms}\} \tag{B3}$$

or

$$\frac{\mathrm{D}b(\mathbf{x}_1, \mathbf{x}_2)}{\mathrm{D}t} = -\bar{\nu}(\mathbf{x}_2)\bar{\rho}(\mathbf{x}_1)\frac{\partial a_n(\mathbf{x}_1, \mathbf{x}_2)}{\partial x_{2n}} + \{\text{other terms}\} \tag{B4}$$

We now change to a centered coordinate, $\mathbf{x}$, and a relative coordinate $\mathbf{r}$:

$$\mathbf{x} = \frac{1}{2}(\mathbf{x}_1 + \mathbf{x}_2), \quad \mathbf{r} = \mathbf{x}_1 - \mathbf{x}_2 \tag{B5}$$

Using a Taylor's series to approximate the mean single-point quantities at the center coordinate gives:

$$\frac{\mathrm{D}b(\mathbf{x}, \mathbf{r})}{\mathrm{D}t} = \sum_{j=0}^{\infty}\left\{\left[-\frac{r_1}{2}\frac{\partial}{\partial x_1}\right]^j\bar{\nu}(\mathbf{x})\right\}\sum_{j=0}^{\infty}\left\{\left[+\frac{r_1}{2}\frac{\partial}{\partial x_1}\right]^j\bar{\rho}(\mathbf{x})\right\}\left\{-\frac{1}{2}\frac{\partial a_n(\mathbf{x}, \mathbf{r})}{\partial x_n} + \frac{\partial a_n(\mathbf{x}, \mathbf{r})}{\partial r_n}\right\} + \{\cdots\} \tag{B6}$$

Under Fourier transformation, this becomes

$$\frac{\mathrm{D}b(\mathbf{x},\mathbf{k})}{\mathrm{D}t} = -\frac{1}{2}\sum_{j=0}^{\infty}\left\{\left[-\frac{i}{2}\frac{\partial}{\partial k_1}\frac{\partial}{\partial x_1}\right]^j\bar{\nu}(\mathbf{x})\right\}\sum_{j=0}^{\infty}\left\{\left[+\frac{i}{2}\frac{\partial}{\partial k_1}\frac{\partial}{\partial x_1}\right]^j\bar{\rho}(\mathbf{x})\right\}\frac{\partial a_n(\mathbf{x},\mathbf{k})}{\partial x_n}$$
$$+\sum_{j=0}^{\infty}\left\{\left[-\frac{i}{2}\frac{\partial}{\partial k_1}\frac{\partial}{\partial x_1}\right]^j\bar{\nu}(\mathbf{x})\right\}\sum_{j=0}^{\infty}\left\{\left[+\frac{i}{2}\frac{\partial}{\partial k_1}\frac{\partial}{\partial x_1}\right]^j\bar{\rho}(\mathbf{x})\right\}ik_n a_n(\mathbf{x},\mathbf{k}) + \{\cdots\} \tag{B7}$$

Now we focus our attention on the second line, letting

$$T(\mathbf{x},\mathbf{k}) = \sum_{j=0}^{\infty}\left\{\left[-\frac{i}{2}\frac{\partial}{\partial k_1}\frac{\partial}{\partial x_1}\right]^j\bar{\nu}(\mathbf{x})\right\}\sum_{j=0}^{\infty}\left\{\left[+\frac{i}{2}\frac{\partial}{\partial k_1}\frac{\partial}{\partial x_1}\right]^j\bar{\rho}(\mathbf{x})\right\}ik_n a_n(\mathbf{x},\mathbf{k}) \tag{B8}$$

or, expanded to second order:

$$T(\mathbf{x},\mathbf{k}) \approx \left\{\bar{\nu}(\mathbf{x})\bar{\rho}(\mathbf{x}) + \frac{i}{2}\left[\bar{\nu}(\mathbf{x})\frac{\partial\bar{\rho}(\mathbf{x})}{\partial x_1} - \bar{\rho}(\mathbf{x})\frac{\partial\bar{\nu}(\mathbf{x})}{\partial x_1}\right]\frac{\partial}{\partial k_1} + \frac{1}{4}\frac{\partial\bar{\nu}(\mathbf{x})}{\partial x_1}\frac{\partial\bar{\rho}(\mathbf{x})}{\partial x_\mathrm{m}}\frac{\partial^2}{\partial k_1\partial k_\mathrm{m}}\right\}ik_n a_n(\mathbf{x},\mathbf{k}) \tag{B9}$$

Now note that on an average over spheres in **k**-space, the first and last terms vanish due to the reality constraint for a_i and the odd order of the powers of k. Thus

$$T(\mathbf{x},\mathbf{k}) \approx -\frac{1}{2}\left\{\bar{\nu}(\mathbf{x})\frac{\partial\bar{\rho}(\mathbf{x})}{\partial x_1} - \bar{\rho}(\mathbf{x})\frac{\partial\bar{\nu}(\mathbf{x})}{\partial x_1}\right\}\int\frac{\partial k_n a_n(\mathbf{x},\mathbf{k})}{\partial k_1}\frac{k^2\,\mathrm{d}\Omega_k}{(2\pi)^3} \tag{B10}$$

A model for the integral term could be

$$\int\frac{\partial k_n a_n(\mathbf{x},\mathbf{k})}{\partial k_1}\frac{k^2\,\mathrm{d}\Omega_k}{(2\pi)^3} \approx C'_{\mathrm{fB}}\delta_{\ln}\frac{\partial k a_n(\mathbf{x},\mathbf{k})}{\partial k} = C'_{\mathrm{fB}}\frac{\partial k a_1(\mathbf{x},\mathbf{k})}{\partial k} \tag{B11}$$

so

$$T(\mathbf{x},\mathbf{k}) \approx -C'_{\mathrm{fB}}\frac{1}{2}\left\{\bar{\nu}(\mathbf{x})\frac{\partial\bar{\rho}(\mathbf{x})}{\partial x_1} - \bar{\rho}(\mathbf{x})\frac{\partial\bar{\nu}(\mathbf{x})}{\partial x_1}\right\}\frac{\partial k a_1(\mathbf{x},\mathbf{k})}{\partial k} \tag{B12}$$

Note that

$$\bar{\nu}(\mathbf{x})\frac{\partial\bar{\rho}(\mathbf{x})}{\partial x_1} - \bar{\rho}(\mathbf{x})\frac{\partial\bar{\nu}(\mathbf{x})}{\partial x_1} = \bar{\nu}^2(\mathbf{x})\frac{\partial}{\partial x_1}\left(\frac{\bar{\rho}(\mathbf{x})}{\bar{\nu}(\mathbf{x})}\right) \tag{B13}$$

so that

$$T(\mathbf{x},\mathbf{k}) \approx -C_{\mathrm{fB}}\left\{\bar{\nu}^2(\mathbf{x})\frac{\partial}{\partial x_1}\left(\frac{\bar{\rho}(\mathbf{x})}{\bar{\nu}(\mathbf{x})}\right)\right\}\frac{\partial k a_1(\mathbf{x},\mathbf{k})}{\partial k} \tag{B14}$$

where

$$C_{\mathrm{fB}} = \frac{1}{2} C'_{\mathrm{fB}} \tag{B15}$$

The form of this term used in this report is equivalent to the above form.

Appendix C

C.1. Spectral behavior of the terms

As compared with decaying constant density homogeneous turbulence, the added difficulty of inhomogeneity and variable density modify the spectral behavior of R_{ij}. The additional variables that are a consequence of the variable density, namely a_i and b, also contribute to altering the spectral shape of R_{ij}. In this Appendix we examine the influence that these variables have on the spectra. We first address the complexities associated with inhomogeneous turbulence and then discuss the resulting alterations in the spectra by splitting the spectra into two sections: (1) the high wave numbers, and (2) the low wave numbers. For each section we identify the terms in the model that have the greatest influence on the behavior of the spectra. For each of the terms, we discuss how they interact with other terms in order to alter the spectrum.

In this Appendix we show the basis for numerous deviations from simple self-similarity for inhomogeneous variable density circumstances. Article II, nevertheless describes a possible set of moment equations based on self-similarity. To proceed with this discussion, however, we will comment on the specific ways in which we can characterize the spectrum associated with the quantities of our model for variable density turbulence.

Here we state the general principal that we follow for this study based on our beliefs about the nature of the attainment and subsistence of the structure of spectral self-similarity: the entire evolution of spectral self-similarity is the direct result of a competition of processes that drive a flow. For the case of the decay of isotropic constant-density homogeneous turbulence, the identification of these competing processes is very simple and straightforward. For this discussion we consider how the turbulent kinetic energy spectrum E, where $E = E_{11} + E_{22} + E_{33}$, is altered only by the transfer of energy among different scales. This transfer can be represented by the local diffusion model (Leith, 1967), which accounts for cascade to higher wave numbers as well as the diffusion to both higher and lower wave numbers. For decaying constant density isotropic turbulence, the transfer of energy through the inertial range of the spectrum is conservative.

For constant density homogeneous anisotropic turbulence with a source, such as a homogeneous shear, the balance between processes must also include the source, which in this case is due to the presence of the E_{12} spectrum coupled to the mean flow gradient. The E_{12} spectrum acts as a source to the E spectrum at the smaller wave numbers. Besnard et al. (1996)

show that this is possible due to the fact that, for high wave numbers, the E_{12} spectrum goes as $k^{-7/3}$ and the E spectrum goes as $k^{-5/3}$. Thus we have a source, namely E_{12}, continuously pumping energy into the E spectrum at the lower wave numbers, the conservative cascade of energy to the higher wave numbers, and the final decay of energy at the highest wave numbers. The idea here is that, similar to the isotropic case, once an equilibrium is reached among the different processes, the energy spectrum assumes a self-similar time independent shape.

For inhomogeneous anisotropic constant density turbulence, such as a free shear layer, additional features such as the diffusion, advection, and nonlocal sources to energy in physical space significantly complicate this balance of processes. With these additional features to the flow, account must also be taken for the transfer of energy in physical space. The sources are still predominately at the small wave numbers (i.e. large scales), and the sink is still at the high wave numbers (i.e. small scales).

Anisotropy adds the remaining six components of the Reynolds stress tensor (or three, taking advantage of symmetry) that do not contribute for the case of isotropic turbulence. This feature of the self-similarity is difficult to represent schematically. The coupling of these components with one another and the exchange of energy that occurs between them also complicate the competition of processes.

For flows that contain a time-dependent source, the characteristic time for the different processes that are responsible for the transfer of energy becomes an issue. For example, if a flow has reached a state of equilibrium between all of its competing processes that transfer energy and the driver of the flow undergoes some type of transient, then the rate of return to equilibrium is governed by a competition between these characteristic times. The processes must compete with one another until an equilibrium is reached and the flow is once again self-similar.

If we now allow the density to vary in the inhomogeneous circumstance, the competition between processes becomes even more involved due to the transfer of energy between the added functions that arise as a consequence of these density fluctuations. Referring to the equations of our model, we see that b drives a_i, which in turn drives R_{ij}. R_{ij} then feeds back into b and a_i through the cascade rates, drag, and the disordered driver of a_i.

As an example of the spectral altering effects of inhomogeneity, consider the turbulent viscosity, υ_t, which is present in the spatial diffusion terms. Letting φ represent any one of the transported turbulence variables, the turbulent viscosity appears in the model equation as

$$\frac{\partial \varphi(k, \mathbf{x}, t)}{\partial t} = \frac{\partial}{\partial x_n} \upsilon_t(\cdots) \frac{\partial \varphi(k, \mathbf{x}, t)}{\partial x_n} + \cdots \tag{C1}$$

The turbulent viscosity can be modeled in either a local (in k-space) version, e.g.

$$\upsilon_t(\mathbf{x}, k, t) = \frac{\sqrt{k R_{nn}}}{k} \tag{C2}$$

which maintains k-dependence; or any one of various types of nonlocal (in k-space) versions, e.g.

$$\upsilon_t(k, \mathbf{x}, t) = \int_0^k \frac{\sqrt{k' R_{nn}}}{(k')^2}\, dk' \tag{C3}$$

and

$$\upsilon_t(\mathbf{x}, t) = \int_0^\infty \frac{\sqrt{k R_{nn}}}{k^2}\, dk \tag{C4}$$

the first of which maintains k-dependence and the latter which is independent of k. The second of the two nonlocal versions of υ_t is a consequence of considering the effect of all scales of the turbulence on the random walk process associated with diffusion. This consideration renders the turbulent viscosity independent of k. The first version accounts for only the wave numbers smaller than the point in the spectrum. The local version represents only the influence on the diffusive process due to eddies associated with the same wave number. A third version could be suggested that would account for the action at all wave numbers larger than the wave-number location, suggesting that it is the smaller turbulent structures that influence the diffusive process the most. This type of representation would also be dependent on k.

The point to be emphasized here is the nature of the modeling for the turbulent viscosity, i.e. whether or not it is dependent on the wave number k (roughly associated with the size of the eddies). For the case where υ_t is independent of wave number, the effective diffusion of the transported variable will be a flux proportional to the gradient that remains constant throughout the entire spectrum. For this particular case, as shown in Eq. (C1), the diffusion term has no explicit dependence on k so that $\partial\varphi/\partial t$ has the same spectral form as φ itself, resulting in no alterations of the spectrum due to the diffusion term. Since this sink/source is independent of k, the diffusion term cannot be responsible for locally altering the spectra in any way. Contrarily, if a version of the turbulent viscosity is used which renders υ_t dependent on the wave number k, the variation in the diffusion for a given point in physical y-space for different magnitudes of k will alter the spectral shape of φ. The variation in the level of diffusion in physical space, y, for all the different wave numbers effectively alters the neighboring spectra resulting in different spectral behaviors.

Thus, the two main effects due to the inhomogeneity are (1) lateral spectrum changes as we move in y-space, and (2) the 'inertial range' is altered even at the same point in y-space. That is to say that not only the adjacent spectra are altered, but also the cascade flux in k-space is no longer constant in the 'inertial range.' To illustrate this quantitatively, suppose that the energy tensor, E, behaves like $k^{-5/3}$ through the inertial range. Then the local version of the turbulent viscosity, Eq. (C2), will behave as $k^{-4/3}$ through the inertial range, and since the

form of the diffusion terms in this model is that found in Eq. (C1), a quantity that behaves like $k^{-9/3}$ through the inertial rage will be diffused to the neighboring locations in physical space.

In view of the above behavior, one may ask the question: does this behavior mean that we have lost the type of self-similarity that has been observed for the case of decaying constant-density homogeneous isotropic turbulence (Besnard et al., 1996)? The answer to this question is probably not; a $k^{-5/3}$ spectrum will dominate a $k^{-9/3}$ contribution at higher wavenumbers. We believe that the spectrum evolves to a self-similar shape. The important concept to recognize here is the method used to detect a self-similar evolution of the spectrum and the fact that $k_{\max}$ (the value of k at which the spectrum attains an extremum) exhibits spatial dependence.

In the process of determining if a spectrum is evolving self-similarly, two things must be done to a time sequence of spectral plots: (1) the magnitudes of the spectra are rescaled such that the extremum of the spectra coincide; and (2) the positions of the spectra are rescaled in such a way that all spectra attain their extremum at the same wave number. With these rescalings, the spectra are said to be evolving self-similarly if a time sequence of spectra can be made to overlay one another. The degree to which one may say that the spectrum is evolving self-similarly is the degree to which the overlaid plots coincide.

To rescale spectra such that the maxima coincide, the value of $k_{\max}$ must be known. A feature of this study is the recognition that $k_{\max}$ is a function of the spatial variable y. With this identification of a spatially dependent $k_{\max}$, we can effectively rescale the spectra so as to test for the self-similar behavior of the spectrum as functions of both y and t. This merely amounts to a different rescaling for each position in y-space through the mixing layer.

C.1.1. High wave numbers

We now examine an important characteristic of the a_i spectrum at high wave numbers. It is shown that as a consequence of the decay terms in the a_i equation, the a_i spectrum falls off much more rapidly for high wave numbers than do the spectra for either b or R_{ij}. Since a_i is the principal source to both b and R_{ij}, this behavior of the a_i spectrum results in a source term to b and R_{ij} that is effectively localized to the lower wave numbers. This behavior of the source term is closely aligned with the behavior of the source term due to a near-flow shear in a constant density flow as previously discussed in this Appendix.

The behavior of the high wave-number part of the a_i spectrum is dominated by a competition among four terms in the transport equation of a_i. These four terms are the two source terms, i.e. the $b\nabla\bar{p}$ term and the $R_{in}\nabla\bar{\rho}/\bar{\rho}^2$ term, and the two drag terms, i.e. the $(C_{\mathrm{rp1}}k^2\sqrt{a_n a_n})a_i$ term and the $(C_{\mathrm{rp2}}k\sqrt{kR_{nn}/\bar{\rho}})a_i$ term. A simple analysis of the competing terms in the transport of the a_i equation shows that the high wave-number behavior of a_i will either vary as $k^{-11/6}$ or $k^{-7/3}$, depending on which drag term is dominating. Due to the lack of any drag-like decay terms in the R_{ij} and b equations, the behavior of these quantities is dominated by the condition of nearly constant flux in k-space, so that they scale very nearly as $k^{-5/3}$ for

the high wave numbers (see Article II). To demonstrate the consistency of these conclusions of a_i for high wave numbers, we use the fact that the two source terms in the a_i equation scale as $k^{-5/3}$ and set up a balance among them and the decay terms. For this examination of the high wave numbers, let us represent the vector component a_i as some constant multiplied by a power, m, of k, i.e. $a_i \longrightarrow a_{i,0}k^m$. Likewise, we can closely approximate R_{ij} and b in a similar fashion: $R_{ij} \longrightarrow R_{ij,0}k^{-5/3}$ and $b \rightarrow b_0 k^{-5/3}$.

With these expressions, the resulting balance among the source and decay terms on the right side of the a_i equation is

$$\left(b_0\frac{\partial\bar{p}}{\partial y}+\frac{R_{yy,0}}{\bar{\rho}^2}\frac{\partial\bar{\rho}}{\partial y}\right)k^{-5/3}\approx\left(C_{\mathrm{rp1}}k\sqrt{a_{n,0}a_{n,0}k^{2m}}+C_{\mathrm{rp2}}k\sqrt{\frac{kR_{nn,0}k^{-5/3}}{\bar{\rho}}}\right)a_{y,0}k^m \tag{C5}$$

From this expression, if the C_{rp1} term is dominating, the following balance must exist between the exponents of k: $2(m+1)=-5/3$, from which we see that $m=-11/6$. This is the expected power of the high wave-number behavior of a_i if the C_{rp1} term dominates the decay. If the C_{rp2} term dominates the high wave-number behavior then the following balance is established: $3/2-5/6+\mathrm{m}=-5/3$, from which we see that the power law behavior for the high wave number part of the spectrum for a_i, becomes $m=-7/3$. Numerically we observe this (see Article II) and see that indeed it is the C_{rp2} term that dominates the decay process. (This dominance is also observed in calculations that show considerable insensitivity to the value of C_{rp1} through any reasonable variations of its magnitude.)

Now that we have established that for the self-similar regime, the high wave number for a_i goes as either $k^{-11/6}$ or $k^{-7/3}$, it follows that since b and R_{ij} both go as $k^{-5/3}$ for high wave numbers, a_i is a source that is localized to the low wave numbers for both b and R_{ij}, and the assumption of cascade dominance for them in the inertial range is confirmed. In this manner, this situation is much like any anisotropic flow. Since the source to both the b and the R_{ij} equation is localized to the low wave numbers, there is a region of nearly constant flux through the inertial range for both b and R_{ij} allowing the spectrum to develop into a $k^{-5/3}$ scaling. The flux is constant in this region for b.

We should note however, that if υ_t varies with k, then there is a possible modification to the inertial spectra for b and R_{ij} arising from variations with k of the y-direction diffusive flux (see earlier reference in this Appendix).

Inversely, for high wave numbers, b creates a_i in a $k^{-5/3}$ fashion across the inertial range. However, as stated above, the drag terms of a_i dominate in this region, which drives the spectrum to a behavior more closely dominated by these drag terms.

C.1.2. Low wave numbers

We have seen the effective localization to small wave numbers of the source term to R_{ij} and b due to the decay terms in the a_i equation. We now examine the low wave-number behavior

of the sources to this model. We first examine the source term to the R_{ij} equation and discuss the modifications resulting from the nonlocal extension to this term, which we have implemented into the model. We then describe the low wave-number behavior of the source terms to the a_i and b equation and other terms that play significant roles in the spectral modifications at low wave numbers.

The main source term to the R_{ij} equation is composed of the net mass fluxing velocity, a_i, coupled to the mean pressure gradient, i.e. $\mathbf{a}\nabla\bar{p}$. The form of this term was examined in Appendix A. Past authors of single-point and two-point models have treated this source term due to the mean pressure gradient as a purely local term (Besnard et al., 1987, 1996; Andronov et al., 1982). That is to say, the production of R_{ij} at a point $\mathbf{x}$ is influenced by the mean pressure gradient only at that same position, $\mathbf{x}$. Due to incompressibility, we know that acoustic signals transfer the effects of the mean pressure changes virtually instantaneously throughout the entire fluid, a global mechanism. In our model, in addition to the spectral formulation, we also formulate this source term to R_{ij} nonlocally in physical space (see Appendix A). The formulation of this nonlocal source term is easier to specify for a spectral model as opposed to a single-point model. The nonlocal spectral formulation is chosen to agree with the known spectral behavior for Rayleigh–Taylor analysis at low wave numbers. The additional information regarding length scales resulting from a spectral formulation enhances our ability to capture the global effects due to incompressibility.

However, as compared with a local source term for R_{ij}, a nonlocal source term does change the spectral behavior of the model. The far-reaching effects of the nonlocal term, i.e. the $k|y'-y|$ factor in the exponential of the Q-function as discussed in Appendix A, directly modify the R_{ij} spectrum and indirectly modify the a_i and b spectra through the coupling to R_{nn} in the local cascade rate and through the coupling to R_{yy} in the density gradient source term to a_i.

Here we examine the modifications to the spectral behavior of the model due to the nonlocal source in R_{ij}. We proceed by examining the two-dimensional (y, k) shape of a purely local source to R_{ij} within the TMZ. Since a_i is zero outside of the TMZ (no net mass flux), the local source, $S_{ij}^{\mathrm{L}}(y, k, t)$ to R_{ij} is likewise zero outside of the TMZ. We show the mechanism by which the local source undergoes a spreading over physical space due to the nonlocal

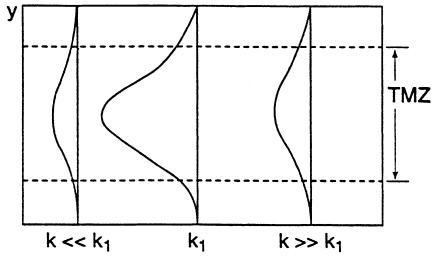

Fig. C1. Schematic of the local source term across the TMZ as a function of y and k. The maximum source corresponds to the wave number k_1 where the spectrum of $a_i(k)$ attains an extremum.

modifications to the local source $S_{ij}^{L}(y, k, t)$ where

$$S_{ij}^{L}(y,k,t) = a_i \frac{\partial \bar{p}}{\partial x_j} + a_j \frac{\partial \bar{p}}{\partial x_i} \tag{C6}$$

Fig. C1 gives a qualitative idea of the nature of the effects of a local source term on $\partial R_{ij}/\partial t$. The wave number k_1 is the wave number at which a_i attains its extremum. The TMZ is shown as the horizontal strip. The drawings across the horizontal TMZ represent, qualitatively, the relative magnitudes of the local source term in the R_{ij} equation. The purpose of these sketches is to depict the influence of the spectral shape of a_i on the source term to $\partial R_{ij}/\partial t$. At $k = k_1$, the contribution to $\partial R_{ij}/\partial t$ of the source term has a maximum while it asymptotes to zero for both the low and high wave numbers of the spectrum. Notice also that the local source term asymptotes to zero at both edges of the TMZ.

We now describe the smearing (across physical space) effect that the incorporation of the nonlocality has on the otherwise local source, $S_{ij}^{L}(y, k, t)$. The nonlocal source is written as

$$\int_{-\infty}^{+\infty} S_{ij}^{L}(y', k, t) Q(y', y, k, t)\, \mathrm{d}y' \tag{C7}$$

We see that the source to R_{ij} at point y receives contributions from S_{ij}^{L}, the local term, integrated over all space; and it is the Q-function that couples the global effects of S_{ij}^{L} back to the point of production. Since the Q-function has the form

$$Q(y', y, k, t) = Q_0(k, t) \exp(-k \mid y' - y \mid) \tag{C8}$$

it will be responsible for altering the shape of the spectrum due to the k dependence. (The $Q_0(k, t)$ is a normalizing function which guarantees a global conservation of the source term over physical space.)

If we first examine only the form of $Q(y', y, k, t)$ uncoupled from the source term, we see that its spectral dependence results in very different forms for large and small values of k.

Fig. C2 shows (qualitatively) the different forms the Q-function will take for different values of k. The structural feature that is important to notice in Fig. C2 is the narrow base width for large values of k as compared with the spread out structures for the smaller values of k. When coupled to S_{ij}^{L}, this feature represents the ability of the large structures of the flow (associated with small k) to reach out and influence remote parts of the flow while the influence due to the smaller structures of the flow (associated with high k) remains highly localized.

Now we couple the local source term, $S_{ij}^{L}(y', k, t)$ to the reaching term, $Q(y', y, k, t)$ and show how the coupling results in a smeared out nonlocal source, $S_{ij}^{NL}(y, k, t)$, to $\partial R_{ij}/\partial t$ that

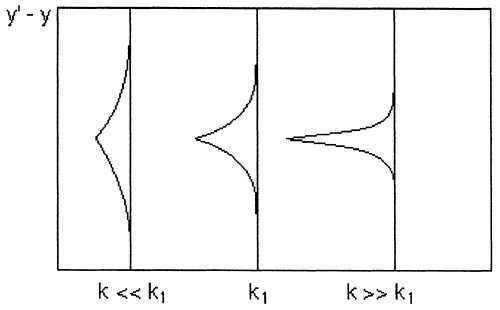

Fig. C2. Schematic representation of the shape of the Q-function. (Notice how the base in the y-direction becomes more narrow for larger values of k.) The area contained by each curve is the same due to normalization.

extends past the edges of the TMZ in physical space. Fig. C3 represents this coupling for a generic value of k.

As before, the smooth hump-like figure represents the local source (Fig. on top), and the new feature to notice is how this local source is smeared out past the edges of the TMZ (figures on bottom). The points at the various y positions outside of the TMZ are used to show the form of the Q-function. (Only a few points are included for clarity.) The point to be made with Fig. C3 is that similar curves for Q exist for all values of y outside of the TMZ, which become more narrow at the base for the larger values of k and widen at the base for smaller values of k. As the integral in the nonlocal source term is performed, contributions are made to $\partial R_{ij}/\partial t$ at positions that lie outside of the TMZ due to the Q-function 'reaching' into the TMZ.

Figs. C2 and C3 show the effect of coupling the Q-function to the local source term to create a nonlocal source term. It is shown that as k gets larger, the width of the base of the Q-function becomes more narrow hence retarding the ability of the nonlocal source term to reach out past the edges of the TMZ. In this limit, the Q-function spreading has little physical basis, and we require only that the result for large k reduce to the local source. Recall that the extremum of the a_i spectrum is at $k = k_1$. The consequence of this feature of the a_i spectrum is

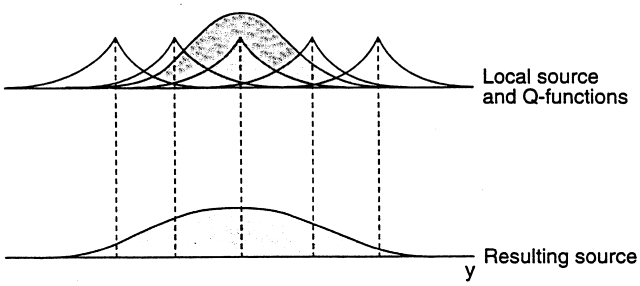

Fig. C3. Schematic representation of the effect of the Q-function on the local source, S_{ij}^{L}, to $R_{ij}(k)$ for a generic wave number.

that the effective local source to $\partial R_{ij}/\partial t$ will be larger for the wave numbers near k_1. The effect of the nonlocality is to flatten the peak of the source near the middle of the TMZ and to extend the source past the edges of the TMZ. The peak of the nonlocal source at the center of the TMZ will always be lower than the peak of the local source due to the normalization

$$\int_{-\infty}^{+\infty} Q(y', y, k, t)\,\mathrm{d}y' = 1 \tag{C9}$$

For small wave numbers, the resulting nonlocal source is spread out over a relatively greater distance in physical space than for the larger wave numbers. This is to weight the nonlocal influence of the larger structures of the flow. Thus, as we traverse the spectrum from $k = 0$ to very large values of k, the a_i spectrum starts at zero, reach a maximum, and then asymptote back to zero; the effect of the nonlocal Q-function on the source is to reach out to infinity for $k = 0$ and asymptote to a local form for very large values of k. When coupled, these two effects produce a source that: (1) is small in magnitude and extends well past the edges of the TMZ in physical space for small values of k; (2) is large in magnitude and is more restricted in physical space for intermediate values of k; and (3) is small in magnitude and completely confined to the TMZ in physical space for asymptotically large values of k.

To summarize Figs. C2 and C3, examine Fig. C4 which compares the local and nonlocal shapes of the $\partial R_{ij}/\partial t$ source term as a function of y for three different ranges of k.

The three plots of Fig. C4 show both the local and nonlocal source as a function of y for different ranges of wave number. The main features of the plots are the decrease in the maximum of the source due to the nonlocality and the distance the nonlocal source extends past the local source as a function of wave number. These three plots of Fig. C4 can now be used to identify spectral modifications near the center and edge of the TMZ. A vertical strip is drawn through the edge of the TMZ as well as the middle of the TMZ ($y = 0$) to help identify the spectral tendency as to how the nonlocal source term modifies the spectral behavior of $\partial R_{ij}/\partial t$. The effect at the edge of the TMZ due to the nonlocality in the source term to $\partial R_{ij}/\partial t$ is an increase in curvature for small wave numbers, an increase in the absolute magnitude of the source as well as a migration of $k_{\max}$ to lower wave numbers. The effect at the center of the TMZ due to the nonlocality in the source term to $\partial R_{ij}/\partial t$ is a decrease in the curvature of the spectrum at the lower wave numbers, a lower absolute magnitude of the source at the centerline, and a migration of $k_{\max}$ to higher wave numbers. This behavior is illustrated in Fig. C5.

The information from Fig. C5 can now be used to determine qualitatively the effects of a nonlocal source on the behavior of $k_{\max}$ through the TMZ. The local source produces a $k_{\max}$ that is concave upward, as a function of y, consistent with the largest turbulent length scales at the centerline of the TMZ (scale = $1/k_{\max}$). The nonlocal source produces a $k_{\max}$ curve through the TMZ that is concave downward, consistent with the larger turbulent length scales found at

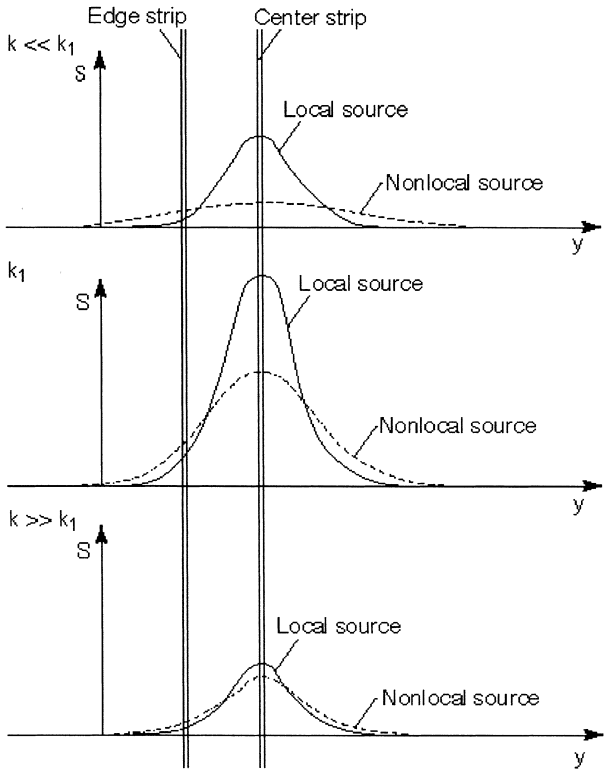

Fig. C4. Schematic to represent the different structures through the TMZ of the nonlocal source term to $\partial R_{ij}/\partial t$ due to the dependence of the nonlocality on wave number k.

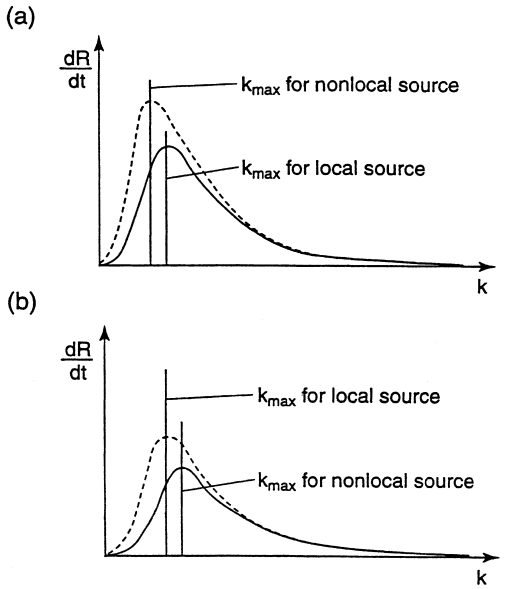

Fig. C5. Schematic representation of the spectral modifications to the time rate of change of the Reynolds stress tensor due to a nonlocal source term for: (a) the edge of the TMZ; and (b) the center of the TMZ.

the edges of the TMZ. Inspection of Fig. 22(c) and (d) of Article II indeed verifies this behavior.

In the limit as $k \to 0$, the value of m is preserved at the initial magnitude. From the nonlocal source term for example with R_{nn} going as $k^m \exp(2t\sqrt{k\mathbf{g}(\rho_2 - \rho_1)/(\rho_1 + \rho_2)})$ for k sufficiently small, this becomes, to leading order, $k^m(1 + 2t\sqrt{k\mathbf{g}(\rho_2 - \rho_1)/(\rho_1 + \rho_2)} + \cdots)$, which shows the preservation of k^m in the limits as $k \to 0$ and also the emergence of a $k^{m+1/2}$ contribution in the spectra from near $k = 0$. This effect can only be visible if C_{fb} is sufficiently small—indeed having a magnitude considerably less than that which is required for agreement with experiment.

In summary, the nonlocal source term to R_{ij} affects the spectrum differently as we traverse the TMZ. Near the centerline of the TMZ the power, m, which dictates the power law behavior of the spectrum, k^m, is decreased for the low wave numbers and only slightly changed at the high wave numbers. Near the centerline, $k_{\max}$ migrates towards higher wave numbers. As we move out towards the edge of the TMZ, the power m is increased for the lower wave numbers, the higher wave numbers are only slightly affected, and $k_{\max}$ migrates to the lower wave numbers. The nonlocal source term to R_{ij} has a major effect on the components of that tensor and are also felt indirectly on a_i and b, principally through the alteration of cascade rates.

Two more items that alter the spectra for the low wave numbers are the initial conditions of b, i.e. the low wave-number initialization for the b spectrum and the C_{fb} term in the b equation. The low wave-number behavior for the b spectrum and the C_{fb} are in constant competition to determine the power law behavior for the low k parts of the spectra. Confined within the b spectrum this competition is most apparent. The C_{fb} term is responsible for a wave-like propagation of the b spectrum from high to low wave numbers. This effect will increase the downward curvature of the b spectrum for the low wave numbers hence lowering the power law, m, of the spectrum where $b \backsim k^m$ for small k. Hence it is apparent that this process will compete with the initial condition of the b spectrum since the spectrum is continually migrating toward smaller wave numbers, thus allowing for a continual influence of the initial conditions. The effect of the C_{fb} term, however, is to always lower the value of m for the low wave-number parts of the b spectrum. The outcome of the competition of these two items then determines the low wave-number behavior for the a_i spectrum that in turn influences the R_{ij} spectrum.

References

Anderson, D.A., Tannehill, J.C., Pletcher, R.H., 1984. Computational Fluid Mechanics and Heat Transfer. Hemisphere, Cambridge, pp. 221–235.

André, J.C., Lesieur, M., 1977. Influence of helicity on the evolution of isotropic turbulence at high Reynolds numbers. J. Fluid Mech. 81, 187–207.

Andronov, V.A., Bakhrakh, S.M., Meshkov, E.E., Nikiforov, V.V., Pevnitshii, A.V., Tolshmyakov, A.I., 1982. An experimental investigation and numerical modeling of turbulent mixing in one-dimensional flows. Sov. Phys. Dokl. 27, 393–396.

Bertoglio, J-P., 1982. A model of three-dimensional transfer in non-isotropic homogeneous turbulence. Bradbury LJS, Durst F, Launder BE, Schmidt FW, Whitelaw JH, Turbulent Shear Flows—3. Springer, Berlin, pp. 253–261.

Bertoglio, J-P., Jeandel, D., 1987. A simplified spectral closure for inhomogeneous turbulence: application to the boundary layer. Bradbury LJS, Durst F, Launder BE, Schmidt FW, Whitelaw JH, Turbulent Shear Flows—5. Springer, Berlin, pp. 19–30.

Besnard, D.C., Harlow, F.H., Rauenzahn, R.M., 1987. Conservation and transport properties of turbulence with large density variations. Los Alamos National Laboratory report LA-10911-MS. Los Alamos, NM, USA. (Also see: Besnard DC, Harlow FH, Rauenzahn RM, Zemach C. 1992. Turbulence transport equations for variable density turbulence and their relationships to two-field models. Los Alamos National Laboratory report LA-12303-MS, Los Alamos, NM, USA.).

Besnard, D.C., Harlow, F.H., Rauenzahn, R.M., Zemach, C., 1992. Turbulence transport equations for variable density turbulence and their relationships to two-field models. Los Alamos National Laboratory report LA-12303-MS. Los Alamos, NM, USA.

Besnard, D., Ducros, F., Loreaux, Ph, Mimouni, S., Vasseur, A., 1995. Turbulent mixing modeling and simulation. In: Glimm J. In:, J. Grove, R. Young (Ed.). Proceedings of 5th International Workshop on the Physics of Compressible Turbulent Mixing. State University of New York, Stony Brook, NY, USA, preprint.

Besnard, D.C., Harlow, F.H., Rauenzahn, R.M., Zemach, C., 1996. Spectral transport model for turbulence. Theoretical and Computational Fluid Dynamics 8, 1–35 (Also see: Besnard DC, Harlow FH, Rauenzahn RM, Zemach C. 1990. Spectral Transport Model for Turbulence. Los Alamos National Laboratory report LA-11821-MS, Los Alamos, NM, USA.).

Bradshaw, P., Cebeci, T., Whitelaw, J.H., 1981. Engineering Calculation Methods for Turbulent Flows. Academic Press, London, pp. 38–49.

Cambon, C., 1979. Modélisation spectrale en turbulence homogène anisotrope. Thèse De Docteur-Ingénieru, Université Claude Bernard, Lyon, France.

Cambon, C., Jeandel, D., Mathieu, J., 1981. Spectral modelling of homogeneous non-isotropic turbulence. J. Fluid Mech. 104, 247–264.

Chandrasekhar, S., 1961. Hydrodynamic and Hydromagnetic Stability. Oxford University Press, Oxford, pp. 428–514.

Chien, K-Y., 1982. Predictions of channel and boundary-layer flows with a low-Reynolds-number turbulence model. AIAA J. 20, 33–38.

Chou, P.Y., 1940. On an extension of Reynolds method of finding apparent stresses and the nature of turbulence. Chin. J. Phys. 4, 1–33.

Clark, T.T., Spitz, P.B., 1995. Two-point correlation equations for variable density turbulence. Los Alamos National Laboratory Report, LA-12671-MS. Los Alamos, NM, USA.

Clark, T.T., Zemach, C., 1995. A spectral model applied to homogeneous turbulence. Phys. Fluids 7, 1674–1694 (Also see: Clark TT. 1992. Spectral self-similarity of homogeneous anisotropic turbulence. Los Alamos National Laboratory report, LA-12284-T, Los Alamos, NM, USA.).

Cranfill, C.W., 1992. A new multifluid turbulent-mix model. Los Alamos National Laboratory report, LA-UR-92-2484. Los Alamos, NM, USA.

Daly, B.J., Harlow, F.H., 1970. Transport equations in turbulence. Phys. Fluids 13, 2634–2649.

Demuren, A.O., Lele, S.K., Durbin, P., 1994. Role of pressure diffusion in non-homogeneous shear flows. In: Bulletin of The American Physical Society Program for the 1994 Annual Meeting of the Division of Fluid Dynamics Vol. 38 (12), 1954.

Godeferd, F.S., Cambon, C., 1994. Detailed investigation of energy transfers in homogeneous stratified turbulence. Phys. Fluids 6, 2084–2100.

Hanjalic, K., Launder, B.E., 1972. A Reynolds stress model of turbulence and its application to thin shear flows. J. Fluid Mech. 52, 609–638.

Hanjalic, K., Launder, B.E., Schiestel, R., 1980. Multiple-time scale concepts in turbulent transport modeling. In: Bradbury L.J.S. In:, F. Durst, B.E. Launder, F.W. Schmidt, J.H. Whitelaw (Ed.). Turbulent Shear Flows—2. Springer, Berlin, pp. 36–49.

Harlow, F.H., Nakayama, P.I., 1967. Turbulence transport equations. Phys. Fluids 10, 2323–2331.

Harlow, F.H., Nakayama, P.I., 1968. Transport of turbulence energy decay rate. Los Alamos Scientific Laboratory report LA-3854. Los Alamos, NM, USA.

Heisenberg, W., 1948. On the theory of statistical and isotropic turbulence. Proc. R. Soc. London A 195, 402–406.
Ilgebusi, J.O., Spalding, D.B., 1985. An improved version of the K–W model of turbulence. J. Heat Transfer 107, 63–69.
Jeandel, D., Brison, J.F., Mathieu, J., 1978. Modeling methods in physical and spectral space. Phys. Fluids 21, 169–182.
Jones, W.P., Launder, B.E., 1972. The prediction of laminarization with a two-equation model of turbulence. Int. J. Heat Mass Transfer 15, 301–314.
Jones, W.P., Launder, B.E., 1973. The calculation of low-Reynolds-number phenomena with a two-equation model of turbulence. Int. J. Heat Mass Transfer 16, 1119–1130.
Kovasznay, L.S.G., 1948. Spectrum of locally isotropic turbulence. J. Aeronaut. Sci. 15, 745–753.
Kraichnan, R.H., 1958. Irreversible statistical mechanics of incompressible hydromagnetic turbulence. Phys. Rev. 109, 1407–1422.
Kraichnan, R.H., 1959. The structure of turbulence at very high Reynolds numbers. J. Fluid Mech. 5, 497–543.
Kraichnan, R.H., 1964. Decay of isotropic turbulence in the direct-interaction approximation. Phys. Fluids 7, 1030–1049.
Kraichnan, R.H., 1965. Lagrangian-history closure approximation for turbulence. Phys. Fluids 8, 575–598.
Kraichnan, R.H., 1971. An almost-Markovian Galilean-invariant turbulence model. J. Fluid Mech. 47, 512–524.
Kraichnan, R.H., 1972. Test-field model for inhomogeneous turbulence. J. Fluid Mech. 56, 287–304.
Kraichnan, R.H., Spiegel, E.A., 1962. Model for energy transfer in isotropic turbulence. Phys. Fluids 5, 583–587.
Launder, B.E., 1990. Phenomenological modelling: present ... and future?. In: J.L. Lumlet (Ed.). Whither Turbulence? or Turbulence at the Crossroads. Springer, Berlin, pp. 439–485.
Launder, B.E., Spalding, D.B., 1972. Lectures in Mathematical Models of Turbulence. Academic Press, London.
Leith, C.E., 1967. Diffusion approximation to inertial energy transfer in isotropic turbulence. Phys. Fluids 11, 671–673.
Leith, C.E., 1971. Atmospheric predictability and two-dimensional turbulence. J. Atmos. Science 28, 145–161.
Lesieur, M., 1990. Turbulence in Fluids, 2nd ed.. Kluwer Academic, Dordrecht, pp. 146–152.
Markatos, N.C., 1986. The mathematical modelling of turbulent flows. Appl. Math. Modell. 10, 190–220.
Millionshikov, M., 1941. On the theory of homogeneous isotropic turbulence. C. R. (Doklady) Acad. Sci. l'URSS 32, 619–621.
Nagano, Y., Hishida, M., 1987. Improved form of the K–ϵ model for wall turbulent shear flows. J. Fluids Engng 109, 156–160.
Ng, K.H., Spalding, D.B., 1972. Turbulence model for boundary layers near walls. Phys. Fluids 15, 20–30.
Nikiforov, V.V., 1991. Calculation of gravitational turbulent mixing in non-automodel flows. Proceedings of 2nd International Workshop on the Physics of Compressible Turbulent Mixing. Cambridge, UK, pp. 478–496.
O'Brien, E.E., Francis, G.C., 1962. A consequence of the zero fourth cumulant approximation. J. Fluid Mech. 13, 369–382.
Oguara, Y., 1963. A consequence of the zero fourth cumulant approximation in the decay of isotropic turbulence. J. Fluid Mech. 16, 33–40.
Orszag, S.A., 1970. Analytical theories of turbulence. J. Fluid Mech. 41, 363–386.
Proudman, I., Reid, W.H., 1954. On the decay of a normally distributed and homogeneous turbulent velocity field. Phil. Trans. R. Soc. Lond. A247, 163–189.
Rotta, W., 1951. Statistische theorie nichthomogener turbulenz. Z. Physik. 129, 547–572.
Saffman, P.G., 1970. A model for inhomogeneous turbulence. Proc. R. Soc. A 317, 417–433.
Saffman, P.G., Wilcox, D.C., 1974. Turbulence-model predictions for turbulent boundary layers. AIAA J. 102, 541–546.
Sandoval, D.L., 1995. Dynamics of variable density turbulence. Los Alamos National Laboratory report LA-13037-T. Los Alamos, NM, USA.
Steinkamp, M.J., 1996. A spectral model for variable density turbulent mixing. Los Alamos National Laboratory report LA-13123-T. Los Alamos, NM, USA.
Steinkamp, M.J., Clark, T.T., Harlow, F.H., 1995. Stochastic interpenetration of fluids. Los Alamos National Laboratory report LA-13016-MS. Los Alamos, NM, USA.
Tatsumi, T., 1957. The theory of decay process of incompressible isotropic turbulence. Proc. R. Soc. Lond. A239, 16–45.
Youngs, D.L., 1992. A two-dimensional turbulence model based on the equations of multiphase flow. Proceedings of 3rd Zababakhin Scientific Talks. Kyshtym, USSR.